An Entropy-Stable Barotropic-Baroclinic Splitting Method for Multilayer Ocean Models

Nina Aguillon[1], Sophie Hörnschemeyer[2], and Jacques Sainte-Marie[1]

[1]Laboratoire Jacques-Louis Lions,
Sorbonne Université, CNRS, Inria

[2]Institute for Geometry and Practical Mathematics,
RWTH Aachen University

4th Commodore Workshop, 23.09.2026

Motivation

- Multilayer models are frequently used in ocean models.
- Computational cost grow with the number of layers.
- Barotropic-baroclinic splitting was introduced to reduce the computational cost.

Killworth, Webb, Stainforth, Paterson: *J. Phys. Ocean. (1991)*
Higdon, Bennett: *J. Comp. Phys. (1996)*
Hallberg: *J. Comp. Phys. (1997)*

Motivation

- Multilayer models are frequently used in ocean models.
- Computational cost grow with the number of layers.
- Barotropic-baroclinic splitting was introduced to reduce the computational cost.

Aim of this project

Numerical analysis of the splitting in the context of hyberbolic systems and finite volume schemes for an idealized multilayer model in terrain-following coordinates.

Killworth, Webb, Stainforth, Paterson: *J. Phys. Ocean. (1991)*
Higdon, Bennett: *J. Comp. Phys. (1996)*
Hallberg: *J. Comp. Phys. (1997)*

Energy, Entropy, and Dissipative Dynamics
igpm
RWTH AACHEN UNIVERSITY

Motivation

- Multilayer models are frequently used in ocean models.
- Computational cost grow with the number of layers.
- Barotropic-baroclinic splitting was introduced to reduce the computational cost.

Aim of this project

Numerical analysis of the splitting in the context of hyberbolic systems and finite volume schemes for an idealized multilayer model in terrain-following coordinates.

Barotropic

- no z-dependence of velocity field
  $\rightarrow$ classical shallow water equation
- surface waves
- fast dynamics

Killworth, Webb, Stainforth, Paterson: *J. Phys. Ocean. (1991)*
Higdon, Bennett: *J. Comp. Phys. (1996)*
Hallberg: *J. Comp. Phys. (1997)*

Energy, Entropy, and Dissipative Dynamics
igpm
RWTH AACHEN UNIVERSITY

Motivation

- Multilayer models are frequently used in ocean models.
- Computational cost grow with the number of layers.
- Barotropic-baroclinic splitting was introduced to reduce the computational cost.

Aim of this project

Numerical analysis of the splitting in the context of hyberbolic systems and finite volume schemes for an idealized multilayer model in terrain-following coordinates.

Barotropic

- no z-dependence of velocity field
  $\rightarrow$ classical shallow water equation
- surface waves
- fast dynamics

Baroclinic

- z-dependence of velocity field
- slower dynamics

Killworth, Webb, Stainforth, Paterson: *J. Phys. Ocean. (1991)*
Higdon, Bennett: *J. Comp. Phys. (1996)*
Hallberg: *J. Comp. Phys. (1997)*

Energy, Entropy, and Dissipative Dynamics
igpm
RWTH AACHEN UNIVERSITY

Motivation

- Multilayer models are frequently used in ocean models.
- Computational cost grow with the number of layers.
- Barotropic-baroclinic splitting was introduced to reduce the computational cost.

Aim of this project

Numerical analysis of the splitting in the context of hyberbolic systems and finite volume schemes for an idealized multilayer model in terrain-following coordinates.

Barotropic

- no z-dependence of velocity field
  $\rightarrow$ classical shallow water equation
- surface waves
- fast dynamics

Baroclinic

- z-dependence of velocity field
- slower dynamics

Killworth, Webb, Stainforth, Paterson: *J. Phys. Ocean. (1991)*
Higdon, Bennett: *J. Comp. Phys. (1996)*
Hallberg: *J. Comp. Phys. (1997)*

Energy, Entropy, and Dissipative Dynamics
igpm
RWTH AACHEN UNIVERSITY

Multilayer Shallow Water Model

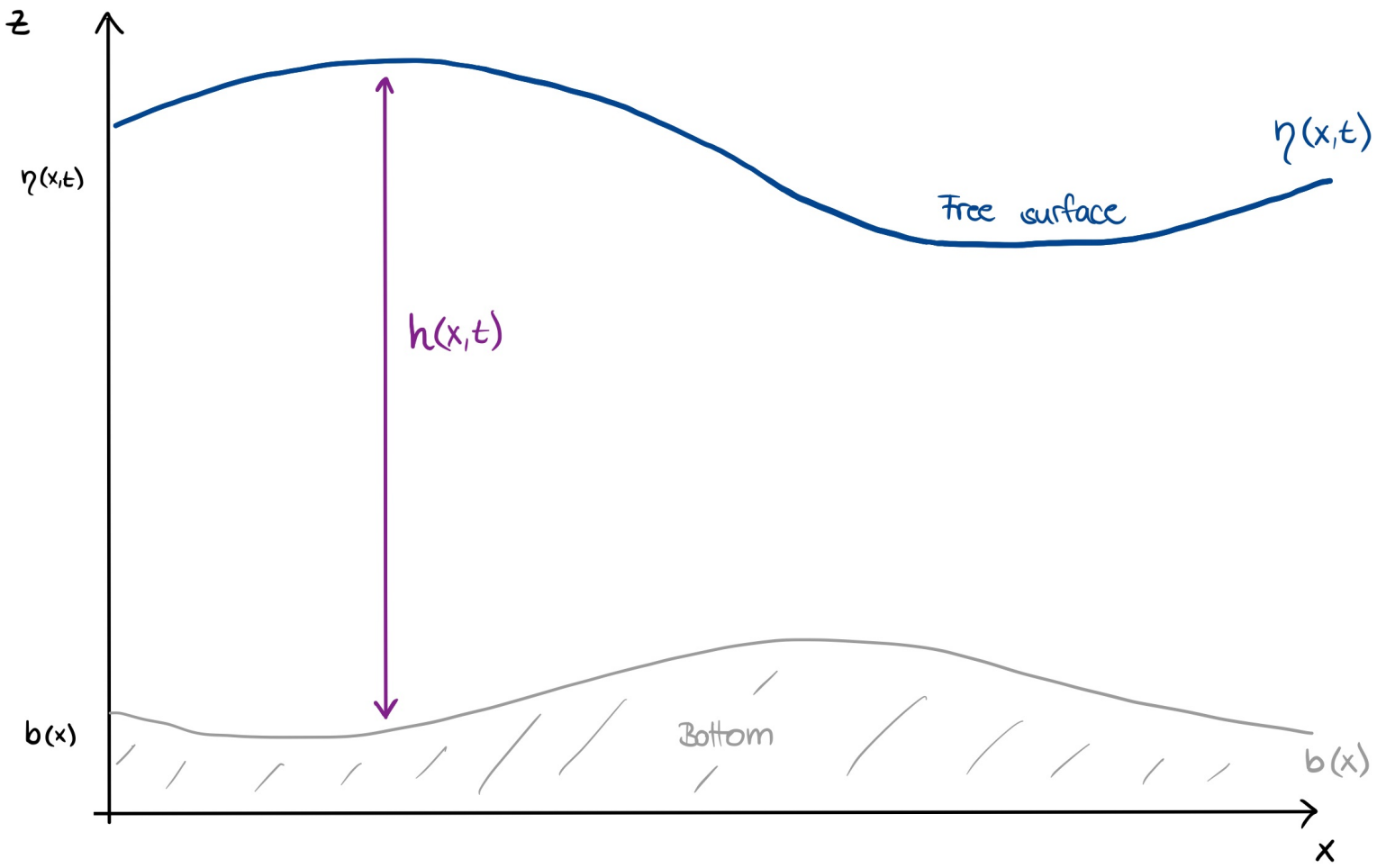

- bottom topography $b(x)$
- free surface $\eta(x,t)$
- water depth $h(x,t)$

Audusse, Bristeau, Perthame, Sainte-Marie: *J. Comp. Phys. (2011)*

Multilayer Shallow Water Model

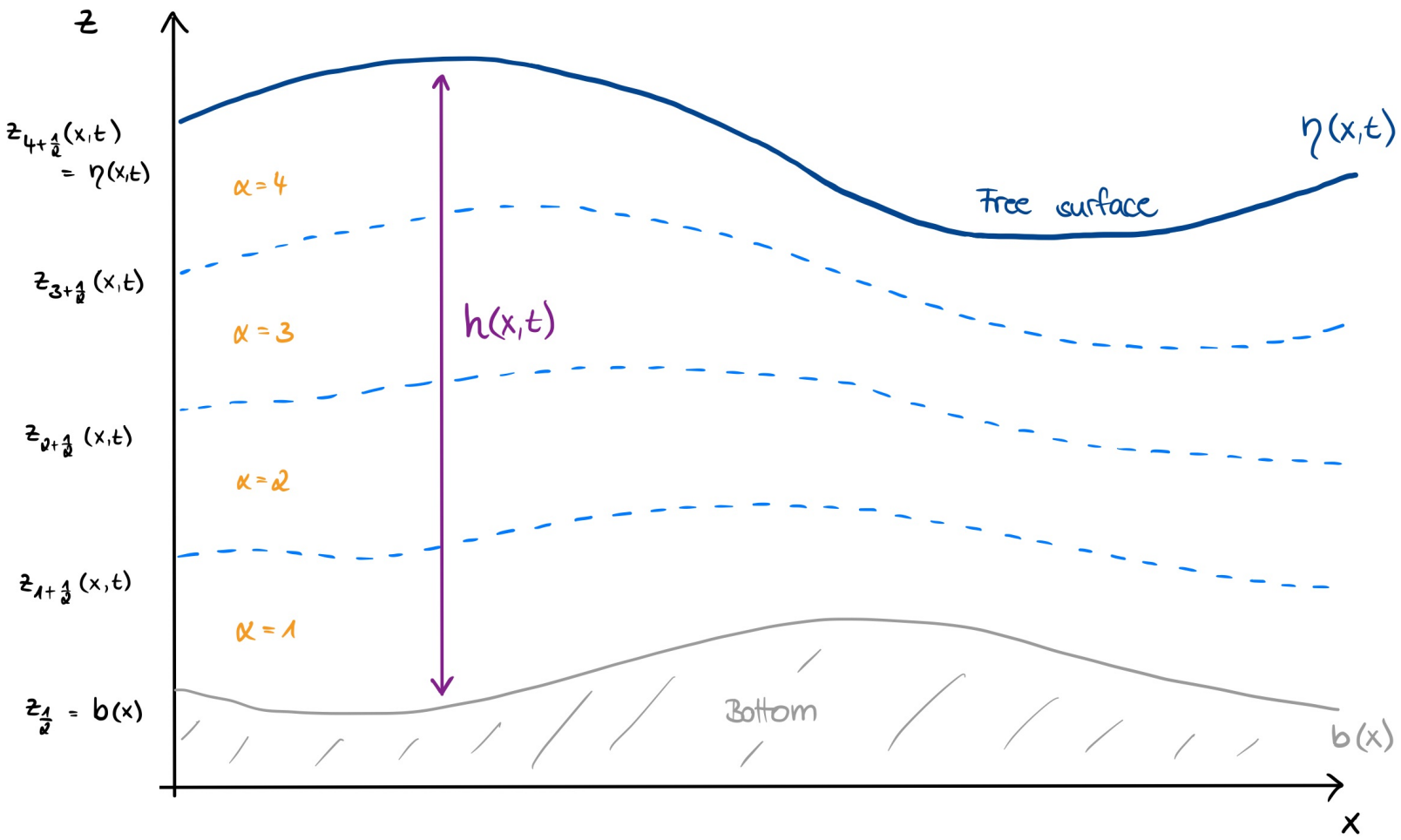

- bottom topography $b(x)$
- free surface $\eta(x,t)$
- water depth $h(x,t)$
- layer thickness ℓ_α with

$$\sum_{\alpha=1}^{N} \ell_\alpha = 1$$

Audusse, Bristeau, Perthame, Sainte-Marie: *J. Comp. Phys. (2011)*

Multilayer Shallow Water Model

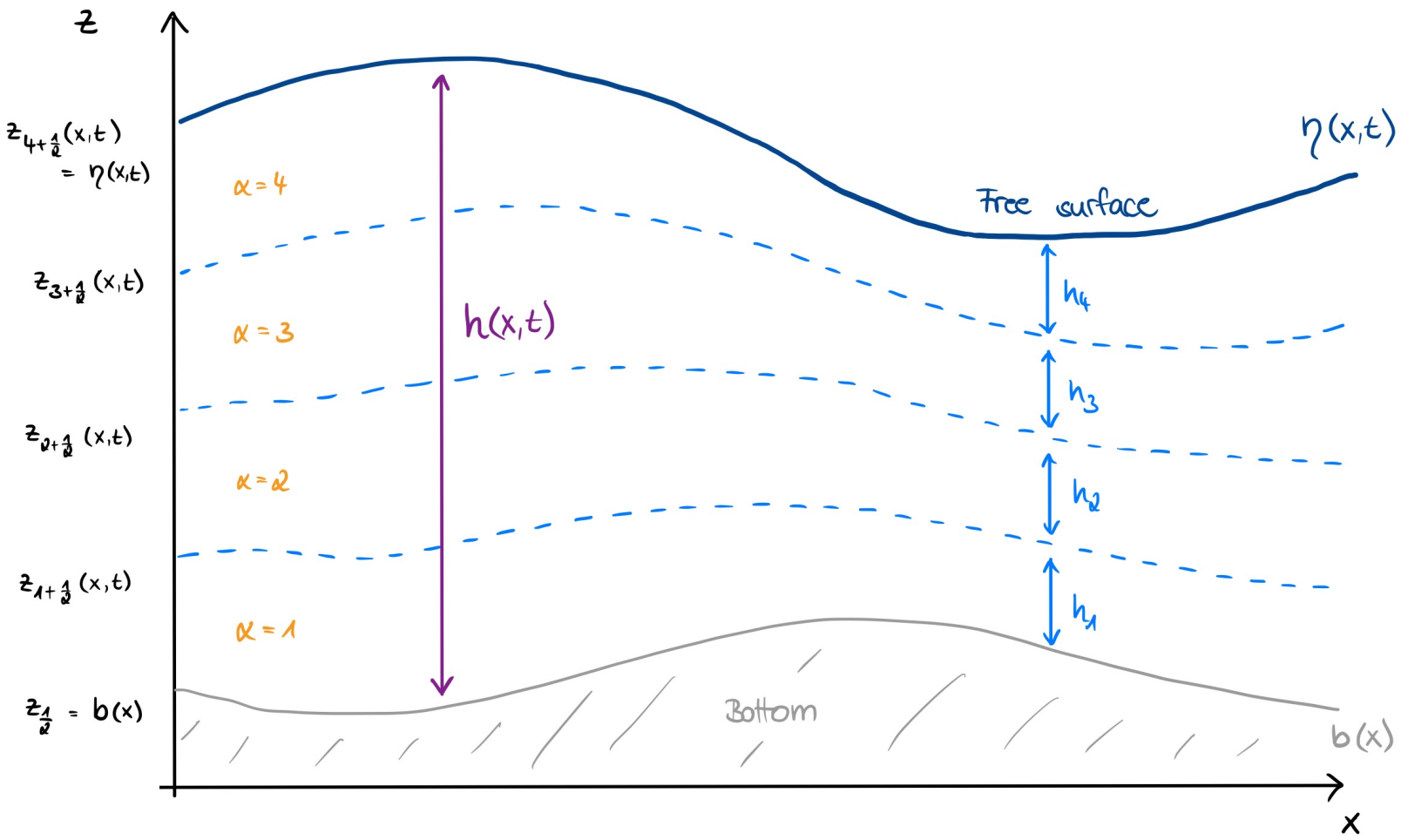

- bottom topography $b(x)$
- free surface $\eta(x,t)$
- water depth $h(x,t)$
- layer thickness ℓ_α with

$$\sum_{\alpha=1}^{N} \ell_\alpha = 1$$

- water height of layer α:

$$h_\alpha(x,t) = \ell_\alpha h(x,t)$$

Audusse, Bristeau, Perthame, Sainte-Marie: *J. Comp. Phys. (2011)*

Multilayer Shallow Water Model

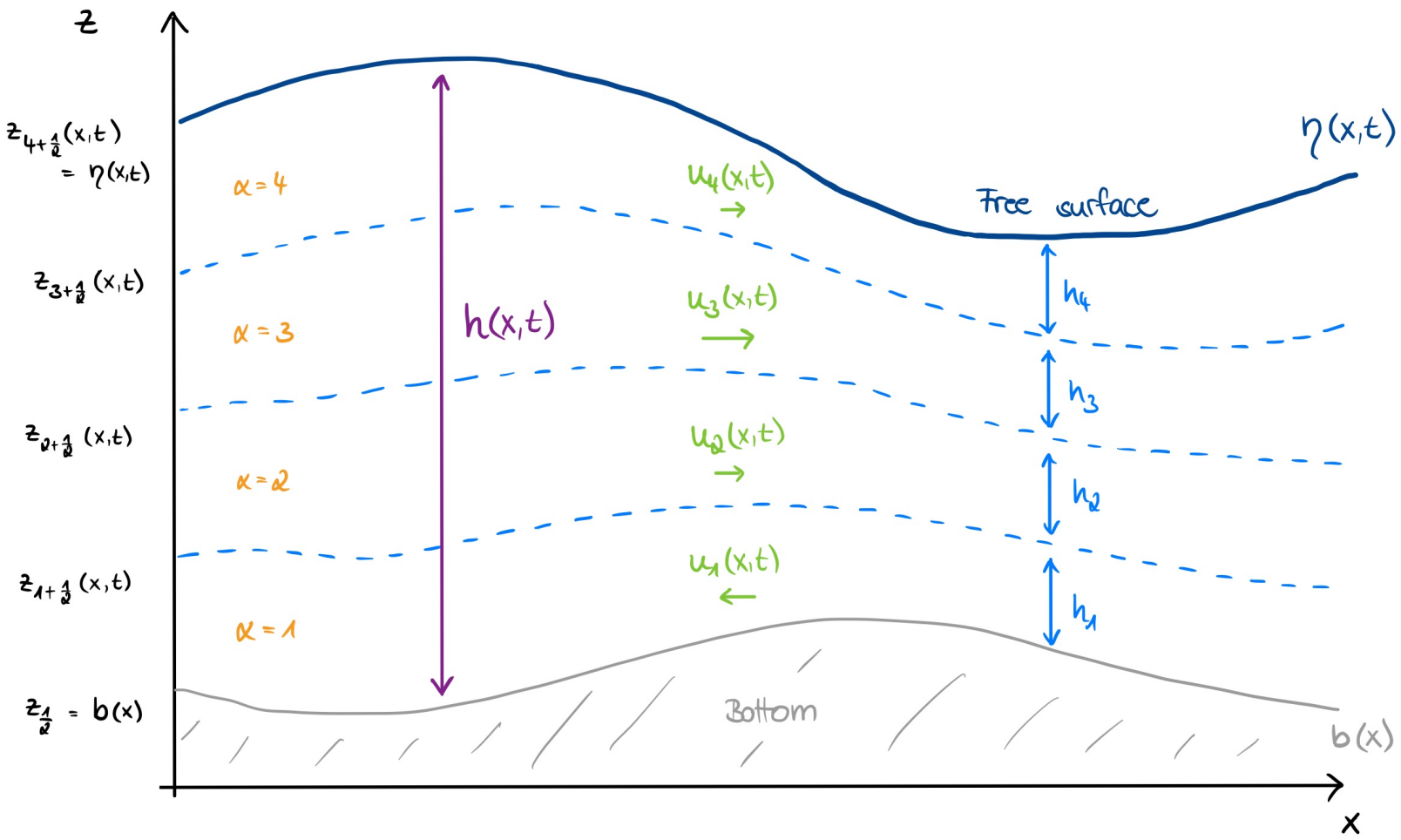

- bottom topography $b(x)$
- free surface $\eta(x,t)$
- water depth $h(x,t)$
- layer thickness ℓ_α with

$$\sum_{\alpha=1}^{N} \ell_\alpha = 1$$

- water height of layer α:

$$h_\alpha(x,t) = \ell_\alpha h(x,t)$$

- layer-averaged velocities $u_\alpha(x,t)$

Audusse, Bristeau, Perthame, Sainte-Marie: *J. Comp. Phys. (2011)*

Multilayer Shallow Water Model

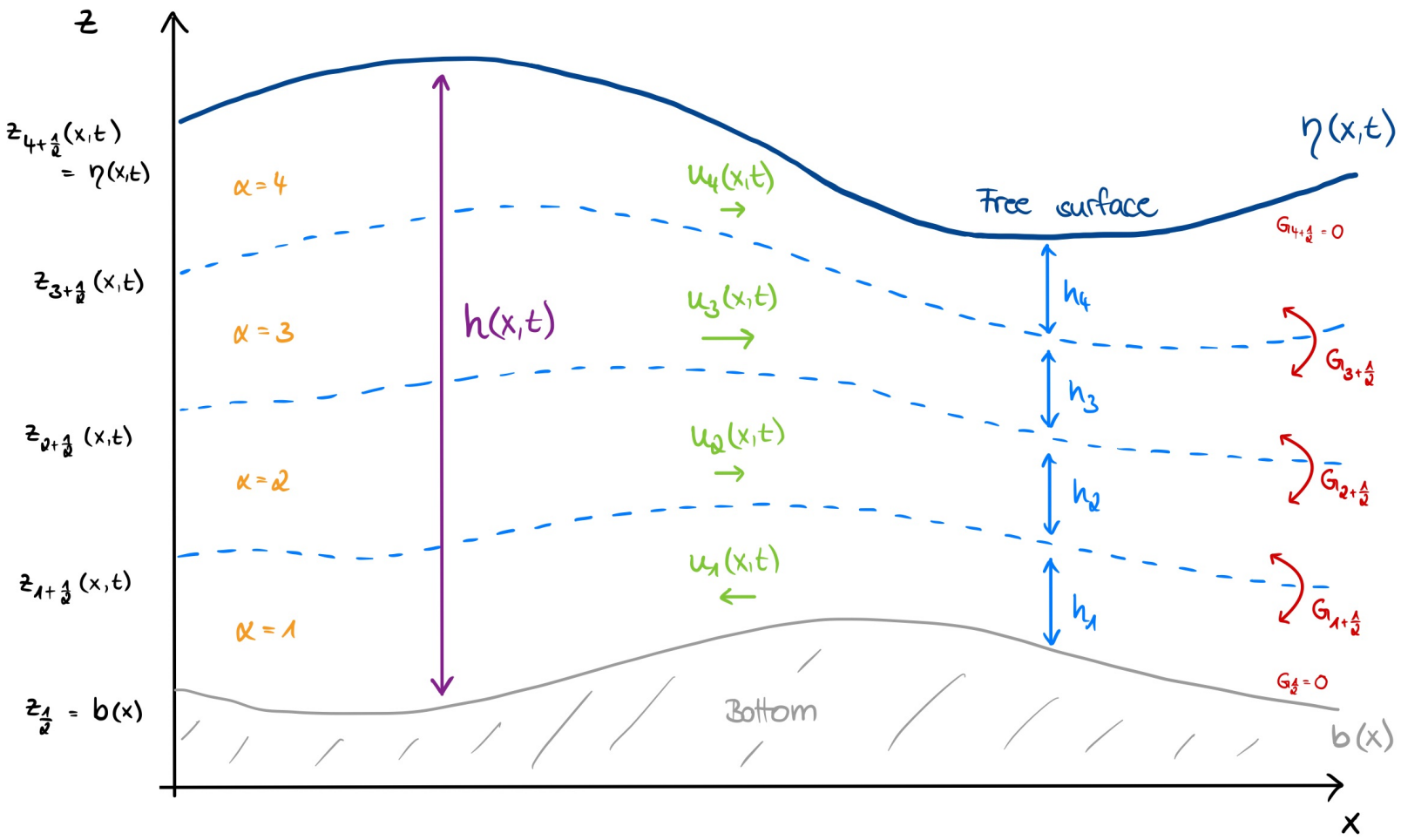

- bottom topography $b(x)$
- free surface $\eta(x,t)$
- water depth $h(x,t)$
- layer thickness ℓ_α with

$$\sum_{\alpha=1}^{N} \ell_\alpha = 1$$

- water height of layer α:

$$h_\alpha(x,t) = \ell_\alpha h(x,t)$$

- layer-averaged velocities $u_\alpha(x,t)$
- mass exchange terms $G_{\alpha\pm\frac{1}{2}}$

Audusse, Bristeau, Perthame, Sainte-Marie: *J. Comp. Phys. (2011)*

Multilayer Shallow Water Model

Multilayer shallow water model with mass exchange

The layer-averaged approximation of the incompressible hydrostatic Euler system with free surface and *constant density* is given by $h_\alpha = \ell_\alpha h$ and

$$\begin{cases} \frac{\partial h}{\partial t} + \sum_{\alpha=1}^{N} \frac{\partial}{\partial x}(h_\alpha u_\alpha) = 0, \\ \frac{\partial}{\partial t}(h_\alpha u_\alpha) + \frac{\partial}{\partial x}(h_\alpha u_\alpha^2 + \frac{1}{2} g h h_\alpha) = -g h_\alpha \frac{\partial b}{\partial x} + u_{\alpha+\frac{1}{2}} G_{\alpha+\frac{1}{2}} - u_{\alpha-\frac{1}{2}} G_{\alpha-\frac{1}{2}} \quad \text{for} \quad \alpha = 1, \dots, N. \end{cases}$$

- mass exchange terms $G_{\alpha+\frac{1}{2}} = \sum_{j=1}^{\alpha} \frac{\partial h_j}{\partial t} + \frac{\partial}{\partial x}(h_j u_j)$
- upwinding strategy for interface velocity

$$u_{\alpha+\frac{1}{2}} = \begin{cases} u_\alpha, & \text{if } G_{\alpha+\frac{1}{2}} \leq 0, \\ u_{\alpha+1}, & \text{if } G_{\alpha+\frac{1}{2}} > 0 \end{cases}$$

- severe timestep restriction

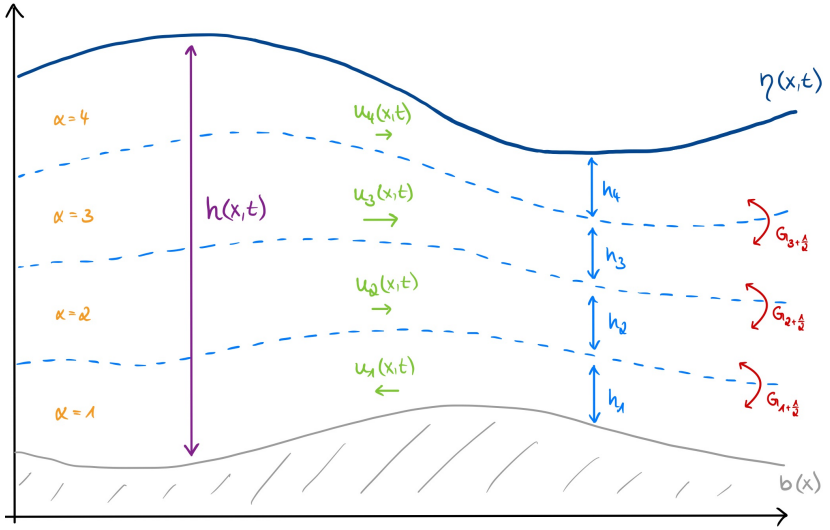

Audusse, Bristeau, Perthame, Sainte-Marie: *J. Comp. Phys. (2011)*

The Splitting: $u_\alpha = \bar{u} + (u_\alpha - \bar{u})$

The Splitting: $u_\alpha = \bar{u} + (u_\alpha - \bar{u})$

Barotropic step

Consists of shallow water equations and advection equation with $\bar{u} = \sum_{\alpha=1}^{N} \ell_\alpha u_\alpha$:

$$\begin{cases} \frac{\partial h}{\partial t} + \frac{\partial}{\partial x}(h\bar{u}) = 0, \\ \frac{\partial}{\partial t}(h\bar{u}) + \frac{\partial}{\partial x}(h\bar{u}^2 + \frac{1}{2}gh^2) = -gh\frac{\partial b}{\partial x}, \\ \frac{\partial}{\partial t}(h(u_\alpha - \bar{u})) + \frac{\partial}{\partial x}(h\bar{u}(u_\alpha - \bar{u})) = 0 \quad \text{for} \quad \alpha = 1, \dots, N. \end{cases}$$

The Splitting: $u_\alpha = \bar{u} + (u_\alpha - \bar{u})$

Barotropic step

Consists of shallow water equations and advection equation with $\bar{u} = \sum_{\alpha=1}^{N} \ell_\alpha u_\alpha$:

$$\begin{cases} \frac{\partial h}{\partial t} + \frac{\partial}{\partial x}(h\bar{u}) = 0, \\ \frac{\partial}{\partial t}(h\bar{u}) + \frac{\partial}{\partial x}(h\bar{u}^2 + \frac{1}{2}gh^2) = -gh\frac{\partial b}{\partial x}, \\ \frac{\partial}{\partial t}(h(u_\alpha - \bar{u})) + \frac{\partial}{\partial x}(h\bar{u}(u_\alpha - \bar{u})) = 0 \quad \text{for} \quad \alpha = 1, \dots, N. \end{cases}$$

Baroclinic step

Contains the vertical exchanges:

$$\begin{cases} \frac{\partial h}{\partial t} = 0, \\ \frac{\partial}{\partial t}(h_\alpha u_\alpha) + \frac{\partial}{\partial x}(h_\alpha u_\alpha(u_\alpha - \bar{u})) = u_{\alpha+\frac{1}{2}} G_{\alpha+\frac{1}{2}} - u_{\alpha-\frac{1}{2}} G_{\alpha-\frac{1}{2}} \quad \text{for} \quad \alpha = 1, \dots, N. \end{cases}$$

Around Hyperbolicity

Reminder:
The largest eigenvalue determines the timestep restriction due to the CFL condition!

Hyperbolicity of barotropic system

$$\lambda^{\mathrm{BT}} = \bar{u}, \bar{u} \pm \sqrt{gh}.$$

Strict hyperbolicity of baroclinic system without exchange terms [AHS'26]

$$\min_{\alpha}(u_\alpha - \bar{u}) \leq \lambda_j^{\mathrm{BC}} \leq \max_{\alpha}(u_\alpha - \bar{u}), \quad j = 1, \ldots, N$$

Note:

$$|\lambda_j^{\mathrm{BC}}| \ll |\lambda_j^{\mathrm{BT}}|.$$

Thus

$$\Delta t^{\mathrm{BC}} \gg \delta t^{\mathrm{BT}}.$$

Aguillon, Hörnschemeyer, Sainte-Marie: *arXiv:2601.16709 (2026)*

Energy, Entropy, and Dissipative Dynamics
igpm
RWTH AACHEN UNIVERSITY

Splitting of Entropy Equality

- physical energy $E = \frac{gh^2}{2} + ghb + \sum_{\alpha=1}^{N} \frac{h_\alpha u_\alpha^2}{2}$ serves as mathematical entropy

Proposition [AHS'26]

Smooth solutions of the **barotropic step** verify the entropy equality

$$\frac{\partial E}{\partial t} + \frac{\partial}{\partial x}\left(gh^2\bar{u} + ghb\bar{u} + \sum_{\alpha=1}^{N} \frac{h_\alpha u_\alpha^2 \bar{u}}{2} \right) = 0.$$

Proposition [AHS'26]

Smooth solutions of the **baroclinic step** verify the entropy equality

$$\frac{\partial E}{\partial t} + \frac{\partial}{\partial x}\left(\sum_{\alpha=1}^{N} \frac{h_\alpha u_\alpha^2 (u_\alpha - \bar{u})}{2} \right) = -\frac{1}{2}\sum_{\alpha=1}^{N} (u_{\alpha+1} - u_\alpha)^2 |G_{\alpha+\frac{1}{2}}|.$$

Aguillon, Hörnschemeyer, Sainte-Marie: *arXiv:2601.16709 (2026)*

Energy, Entropy, and Dissipative Dynamics
igpm
RWTH AACHEN UNIVERSITY

Time Splitting – Lie-Trotter Splitting

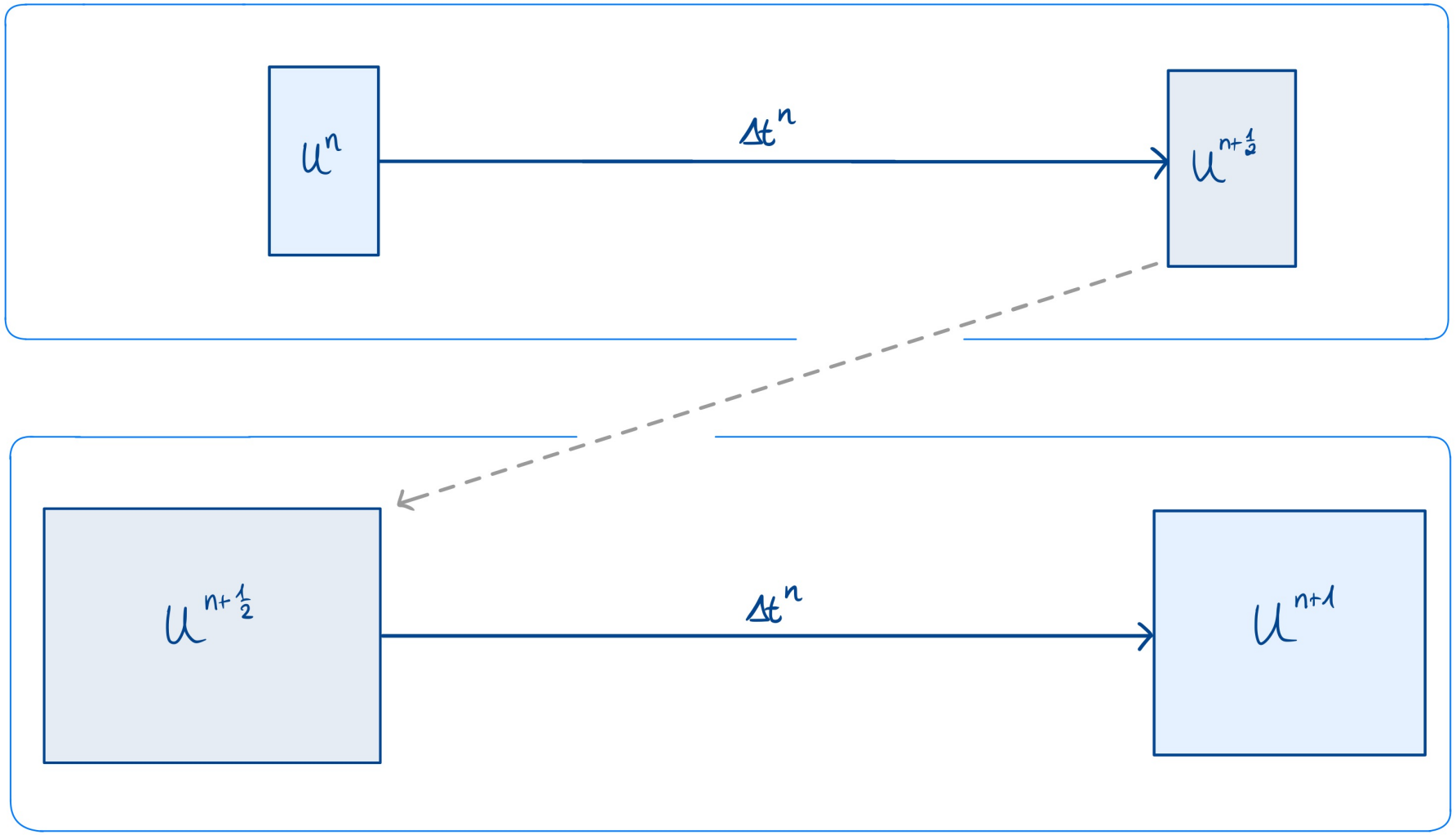

Time Splitting – Lie-Trotter Splitting

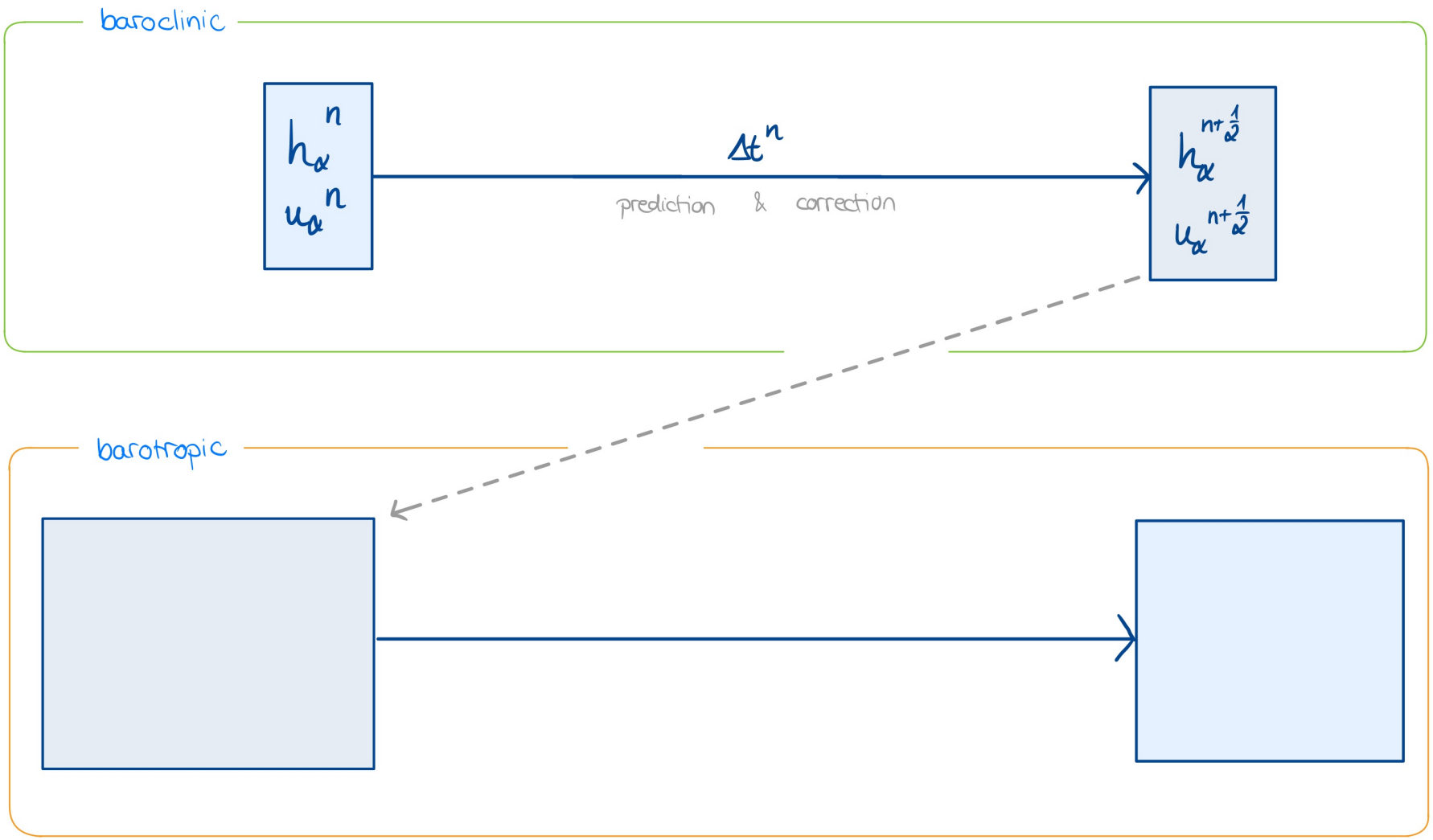

Time Splitting – Lie-Trotter Splitting

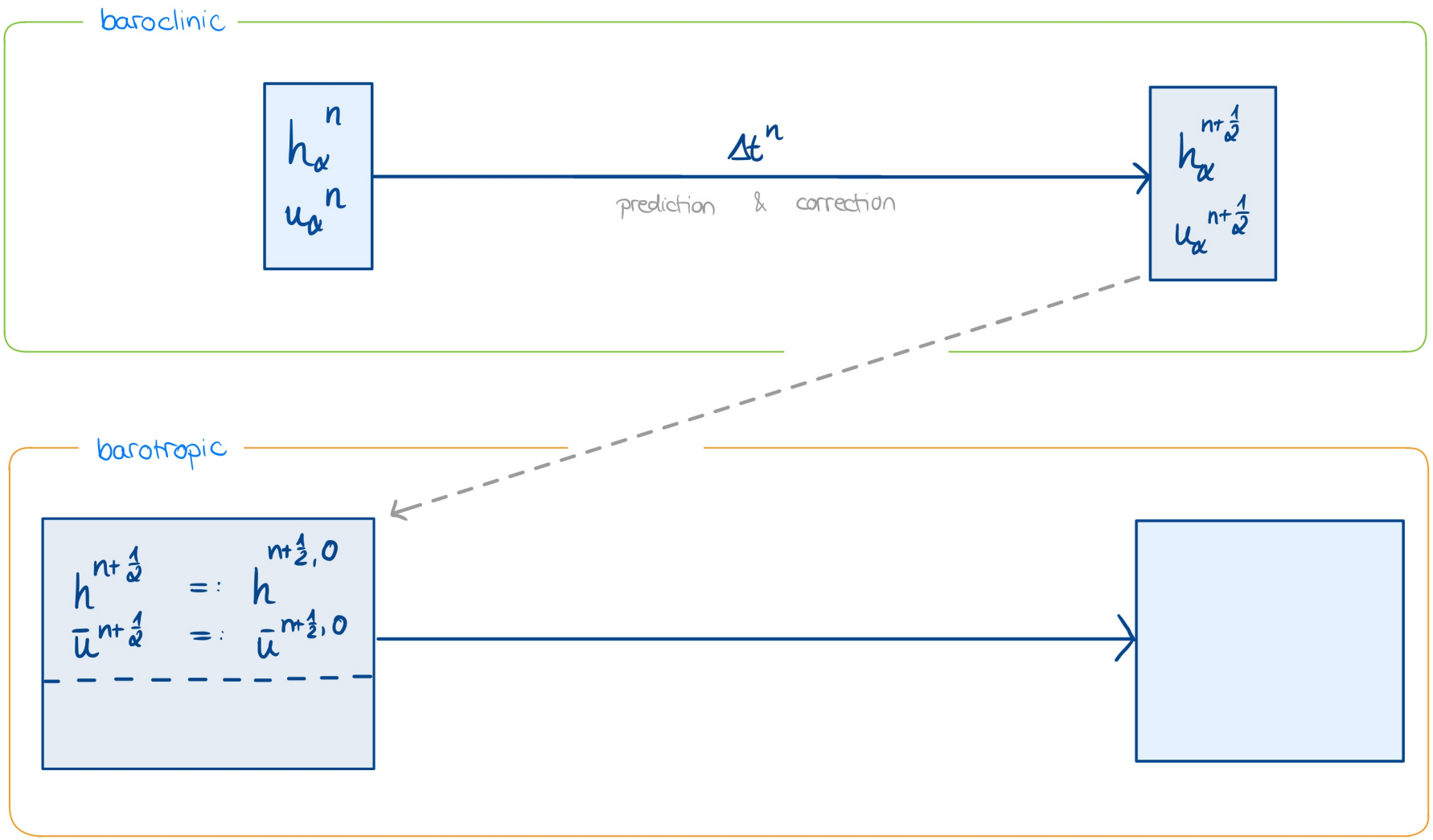

Time Splitting – Lie-Trotter Splitting

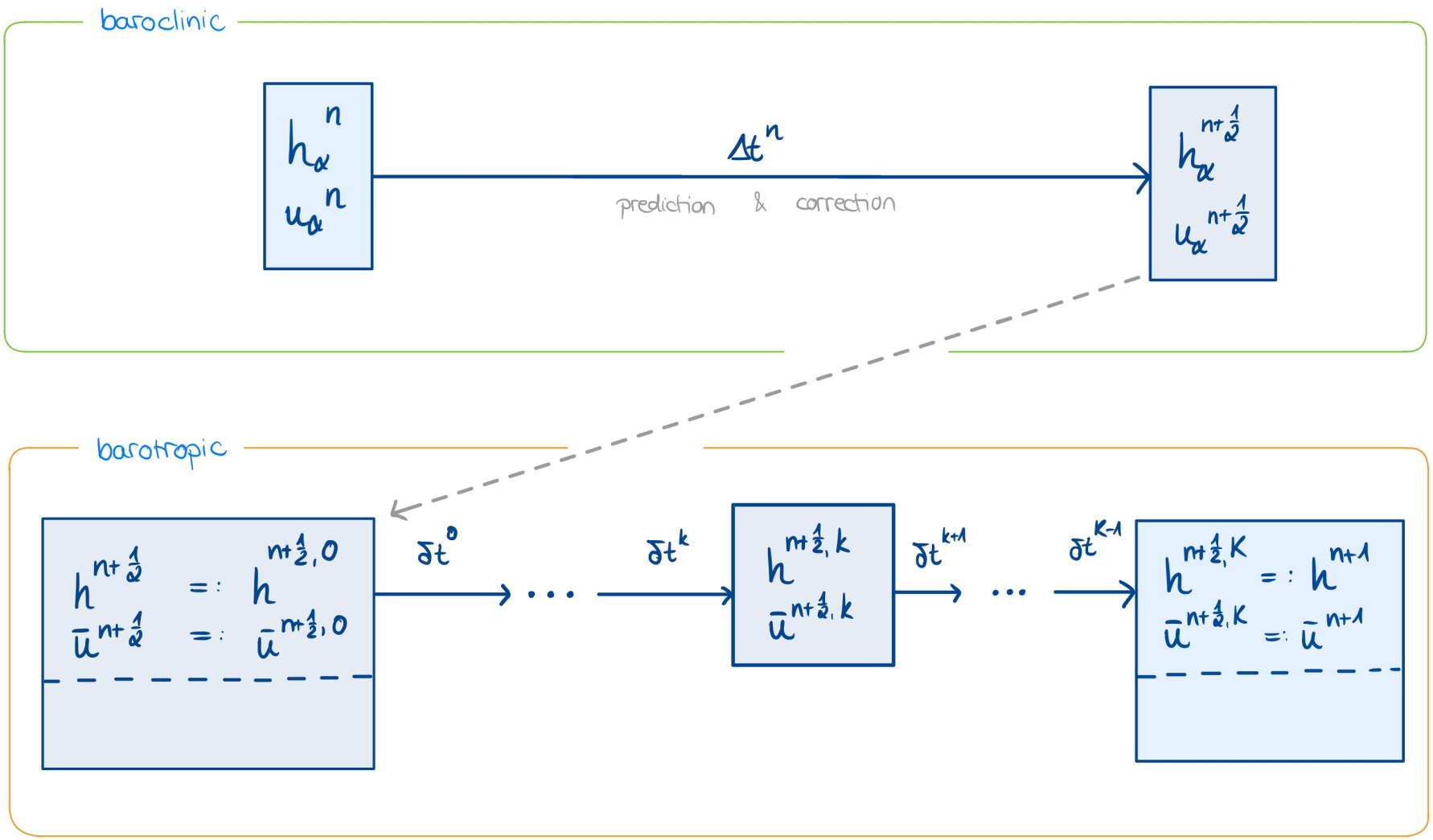

Time Splitting – Lie-Trotter Splitting

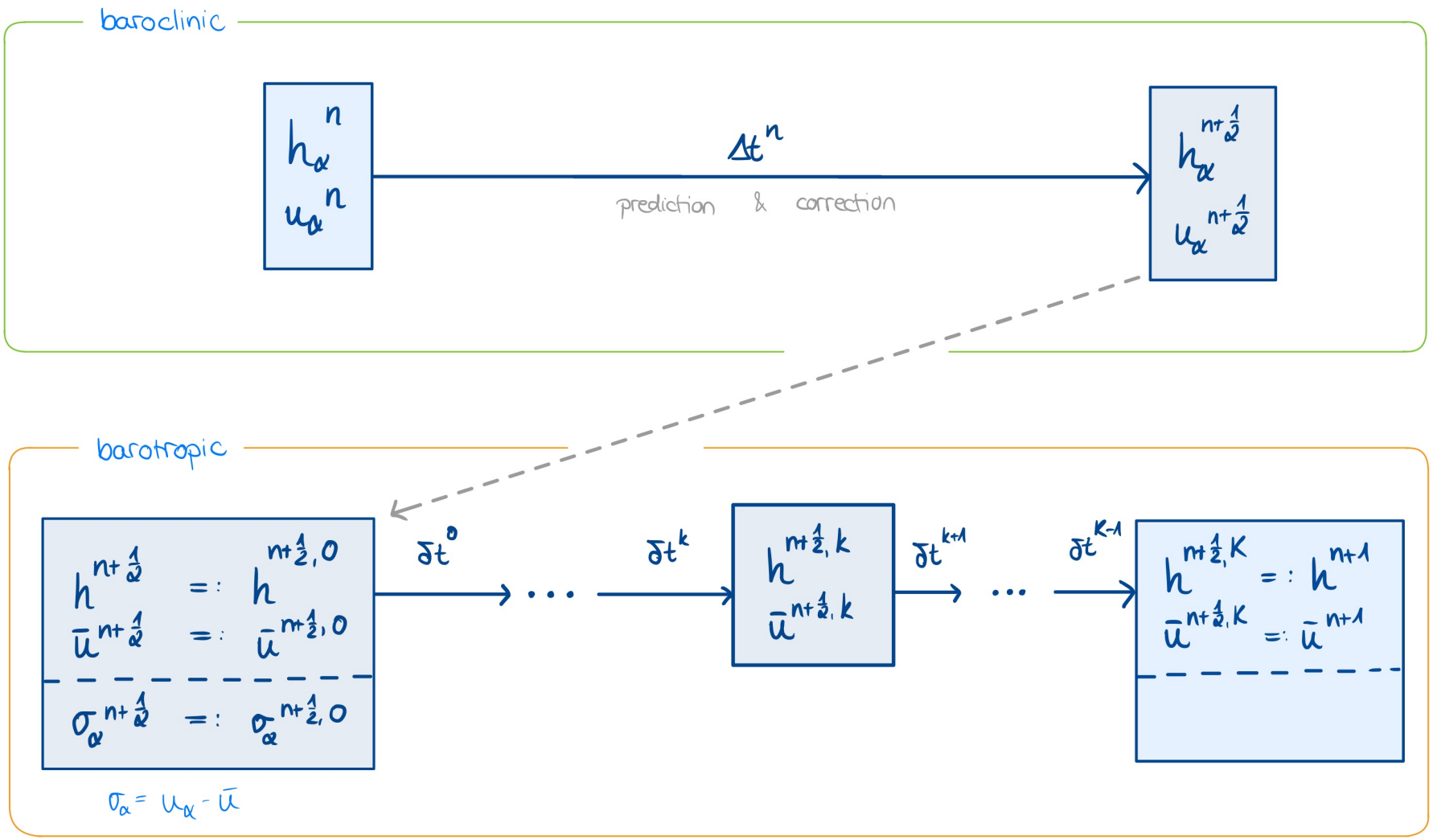

Time Splitting – Lie-Trotter Splitting

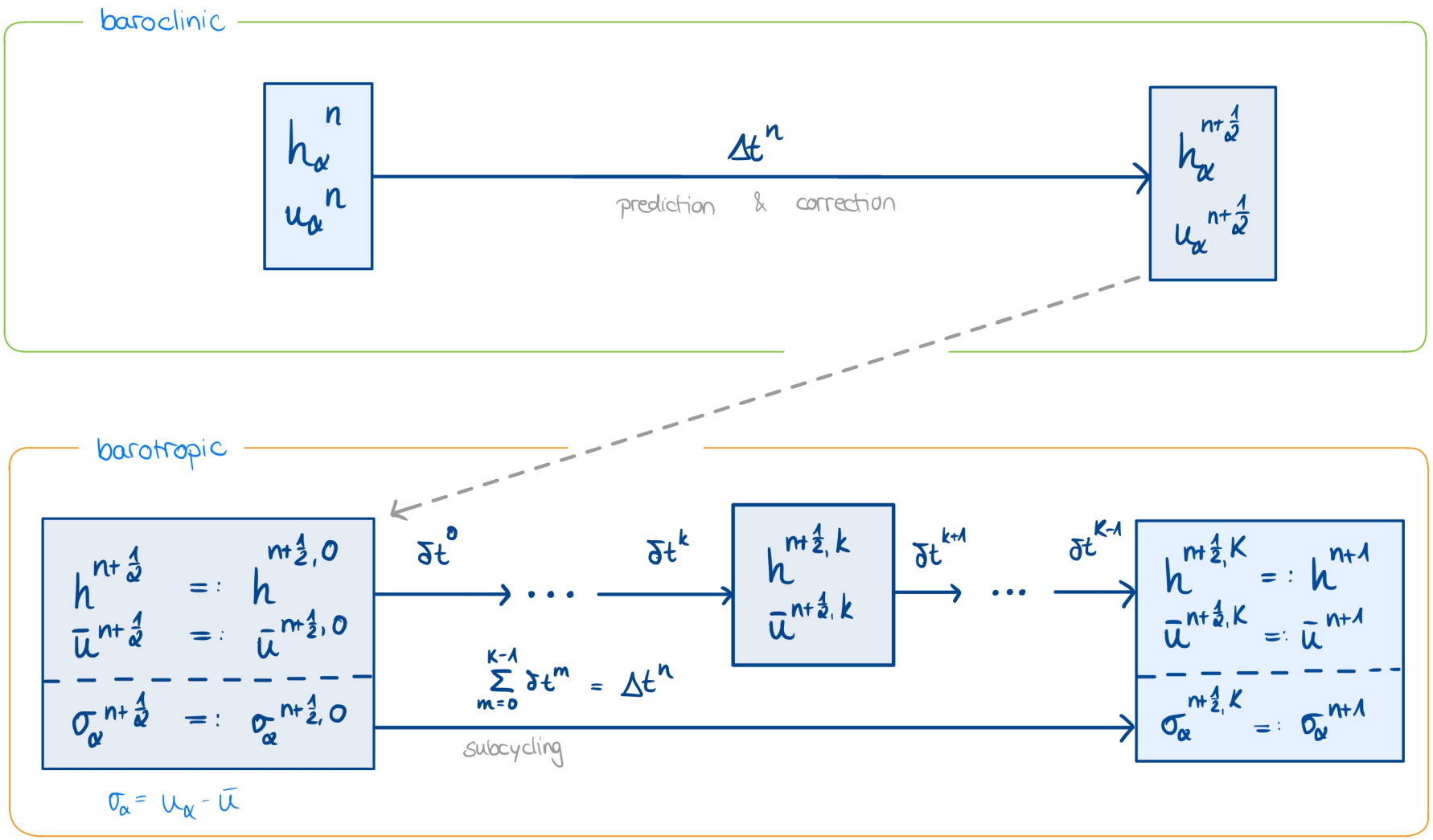

Time Discretization – Baroclinic Step

baroclinic prediction: recall $\sigma_\alpha = u_\alpha - \bar{u}$

$$\begin{pmatrix} h_\alpha \\ h_\alpha u_\alpha \end{pmatrix}^* := \begin{pmatrix} h_\alpha \\ h_\alpha u_\alpha \end{pmatrix}^n - \Delta t^n \frac{\partial}{\partial x} \begin{pmatrix} h_\alpha \sigma_\alpha \\ h_\alpha u_\alpha \sigma_\alpha \end{pmatrix}$$

- mass flux: Rusanov flux
- momentum flux: upwind flux

$$F^{h_\alpha u_\alpha}_{j+\frac{1}{2}} = u^n_{\alpha,j} \left(F^{h_\alpha}_{j+\frac{1}{2}}\right)^+ - u^n_{\alpha,j+1} \left(F^{h_\alpha}_{j+\frac{1}{2}}\right)^-$$

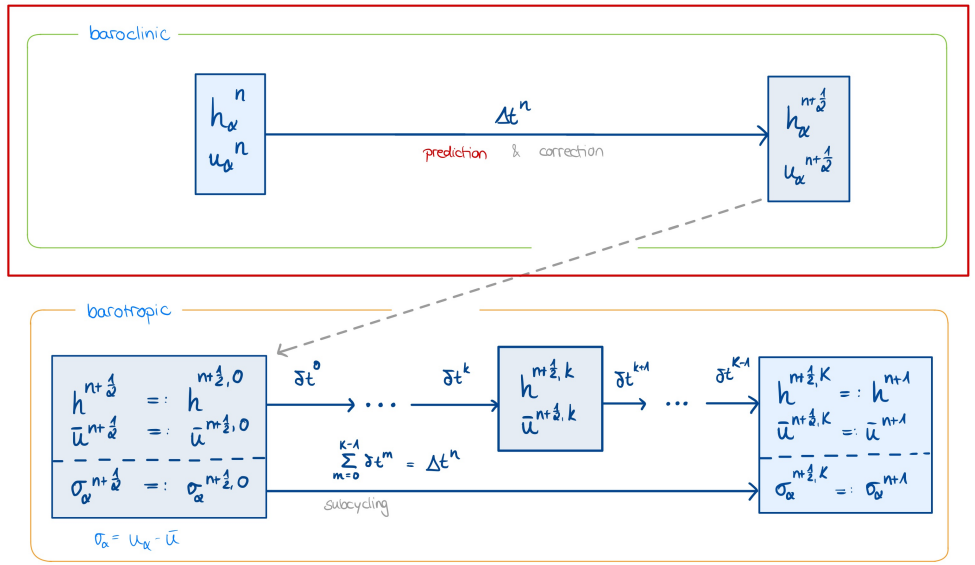

Time Discretization – Baroclinic Step

baroclinic correction:

- proportional water heights:

$$h^{n+\frac{1}{2}} := \sum_{\alpha=1}^{N} h_\alpha^*, \qquad h_\alpha^{n+\frac{1}{2}} := \ell_\alpha h^{n+\frac{1}{2}}$$

- exchange terms:

$$G_{\alpha+\frac{1}{2}} := G_{\alpha-\frac{1}{2}} - \frac{h_\alpha^{n+\frac{1}{2}} - h_\alpha^*}{\Delta t^n} \qquad \text{with} \quad G_{\frac{1}{2}} = 0 = G_{N+\frac{1}{2}},$$

$$(h_\alpha u_\alpha)^{n+\frac{1}{2}} := (h_\alpha u_\alpha)^* + \Delta t^n \left(u_{\alpha+\frac{1}{2}}^{n+\frac{1}{2}} G_{\alpha+\frac{1}{2}} - u_{\alpha-\frac{1}{2}}^{n+\frac{1}{2}} G_{\alpha-\frac{1}{2}} \right)$$

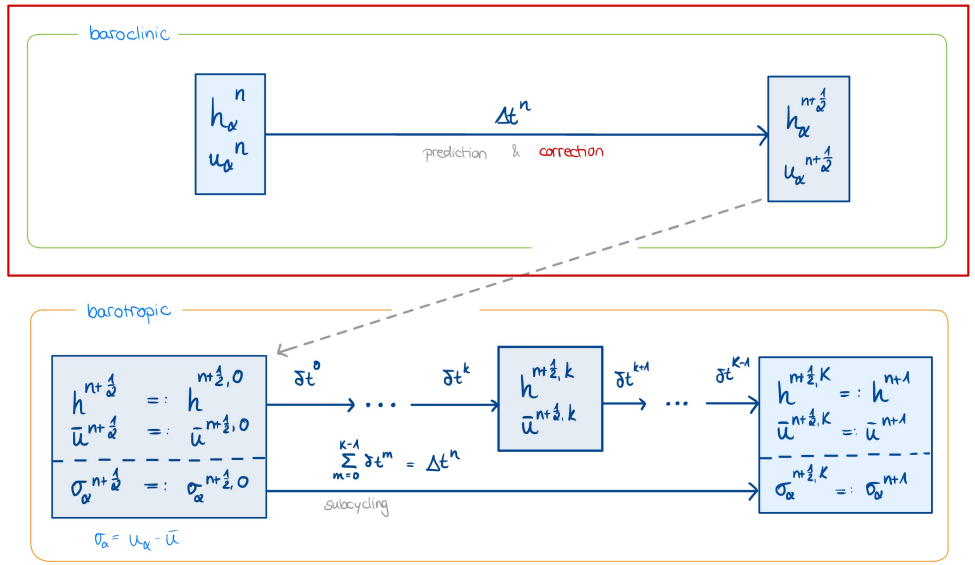

Time Discretization – Barotropic Step

barotropic steps:
many small time steps δt^k s.t. $\sum_{k=1}^{K-1} \delta t^k = \Delta t^n$

- define

$$h^{n+1,0} := h^{n+\frac{1}{2}}, \qquad \bar{u}^{n+1,0} := \bar{u}^{n+\frac{1}{2}}$$

- compute

$$\begin{pmatrix} h \\ h\bar{u} \end{pmatrix}^{n+1,k+1} := \begin{pmatrix} h \\ h\bar{u} \end{pmatrix}^{n+1,k} - \delta t^k \frac{\partial}{\partial x} \begin{pmatrix} h\bar{u} \\ h\bar{u}^2 + \frac{g}{2}h^2 \end{pmatrix} + \delta t^k \begin{pmatrix} 0 \\ gh\frac{\partial b}{\partial x} \end{pmatrix}$$

$$h^{n+1} := h^{n+1,K}, \quad (h\bar{u})^{n+1} := (h\bar{u})^{n+1,K}$$

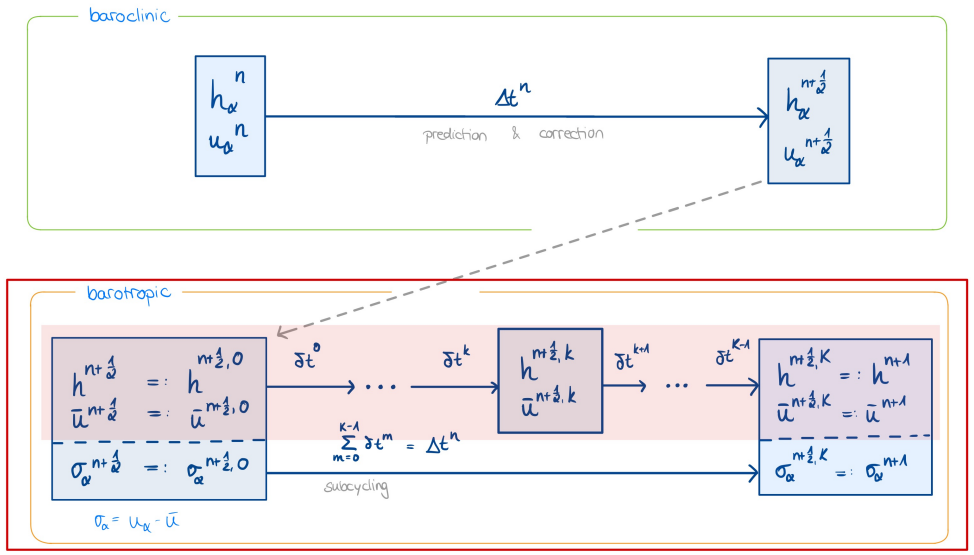

Time Discretization – Barotropic Step

subcycling:

- barotropic mass flux: $f^{h,k}_{j+\frac{1}{2}}$

$$\rightarrow \text{ define } \Delta t^n \mathcal{F}^h_{j+\frac{1}{2}} := \sum_{k=0}^{K-1} \delta t^k f^{h,k}_{j+\frac{1}{2}}$$

- barotropic advection flux: upwind flux

$$\mathcal{F}^{h\sigma_\alpha}_{j+\frac{1}{2}} = \sigma^n_{\alpha,j} \left(\mathcal{F}^h_{j+\frac{1}{2}}\right)^+ - \sigma^n_{\alpha,j+1} \left(\mathcal{F}^h_{j+\frac{1}{2}}\right)^-$$

- update

$$(h\sigma_\alpha)^{n+1} := (h\sigma_\alpha)^n - \Delta t^n \frac{\partial}{\partial x}(h\bar{u}\sigma_\alpha)$$

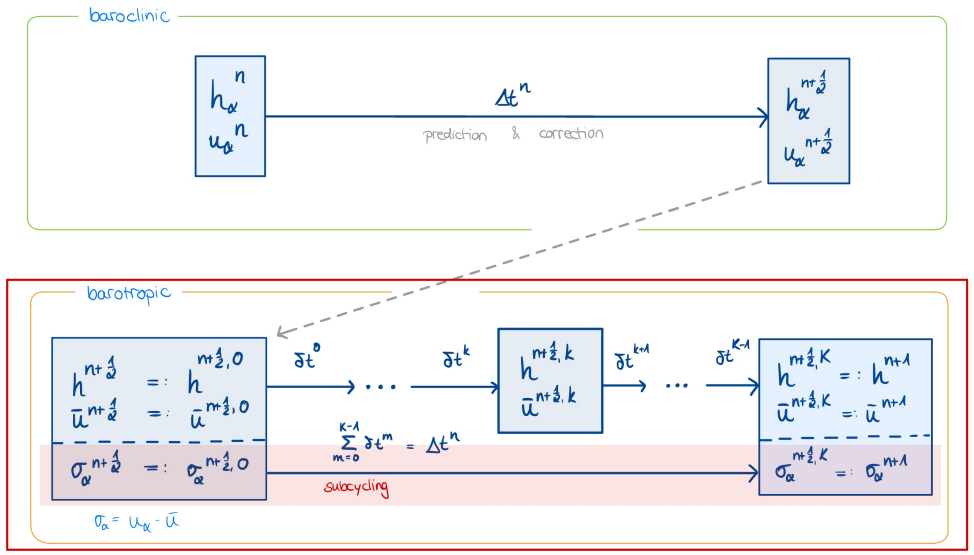

Properties of the Barotropic-Baroclinic Splitting Scheme

Physics:

under classical CFL conditions the scheme

- preserves the non-negativity of the water height
- fulfills a discrete maximum principle for tracers

Numerics:

- inherits the well-balancing property of the shallow water solver
- fulfills a discrete entropy inequality under classical CFL conditions

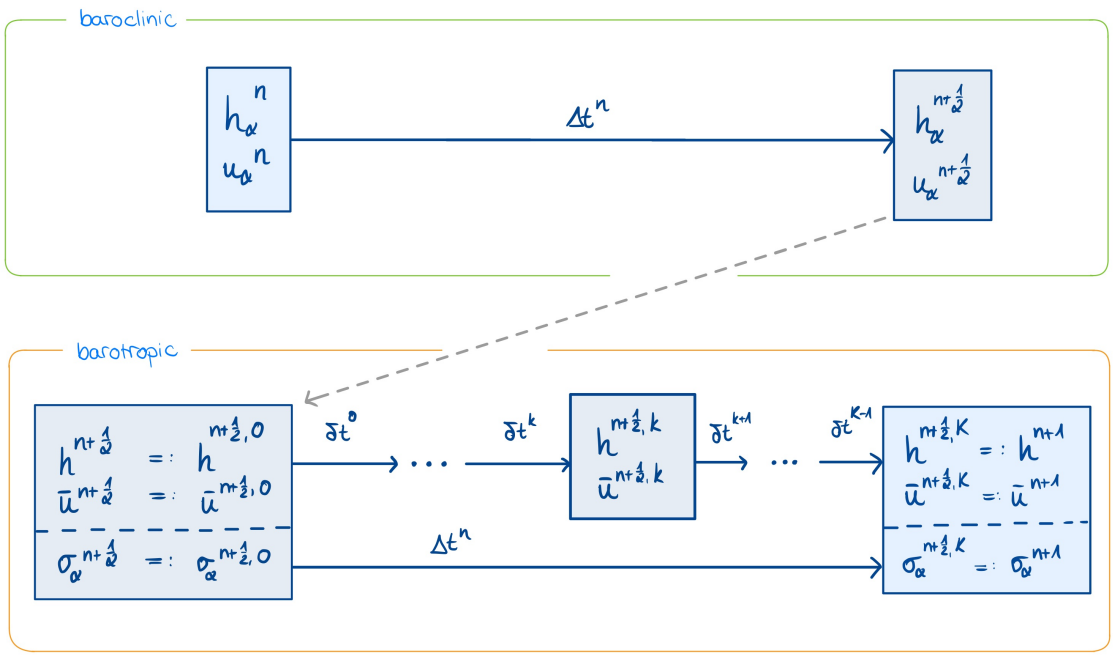

Numerical Experiments – Convergence to Analytical Solution

Stationary analytical solution of Euler equations:

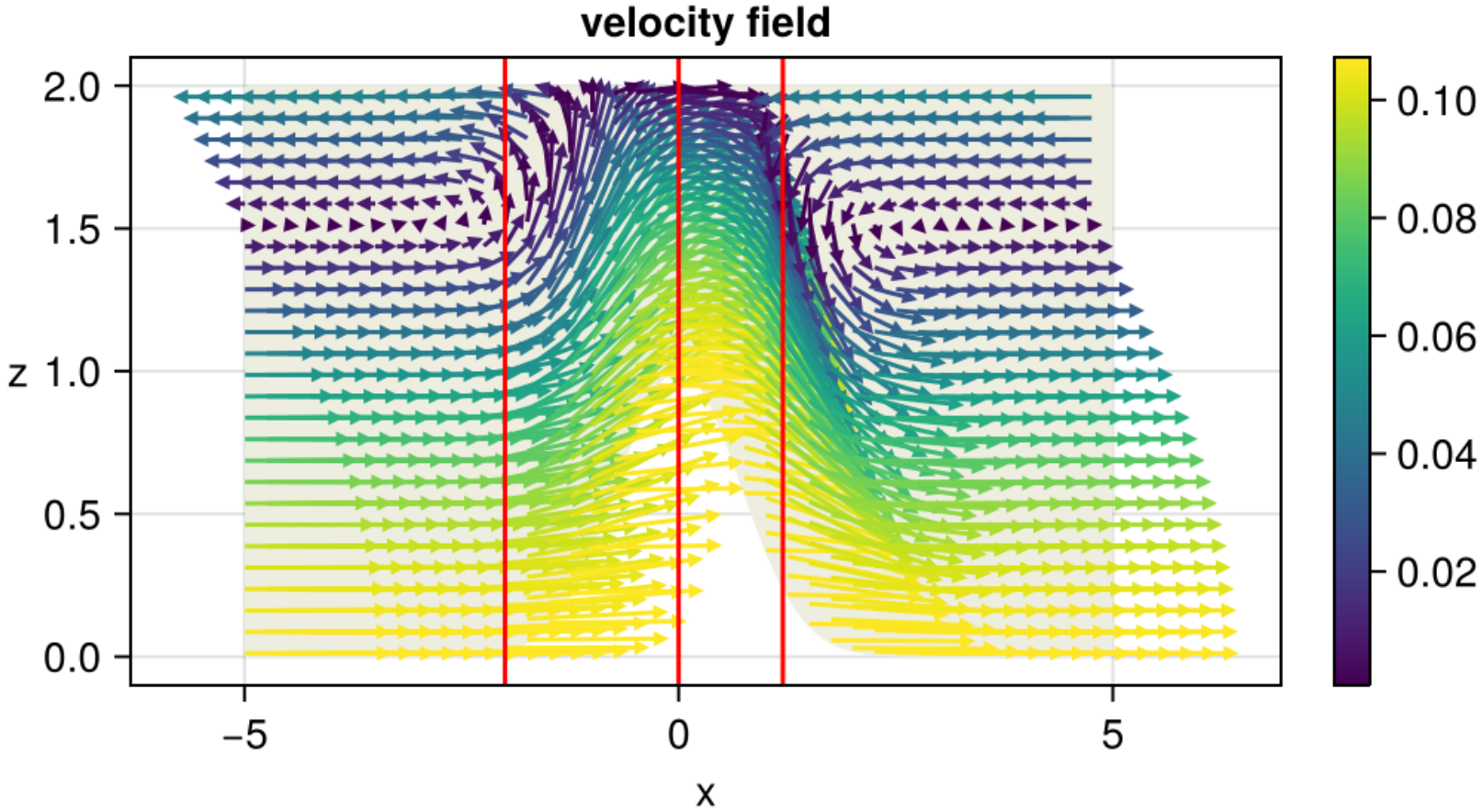

Boulanger, Bristeau, Sainte-Marie: *Comm. Math. Sci. (2013)*

Numerical Experiments – Convergence to Analytical Solution

Stationary analytical solution of Euler equations:

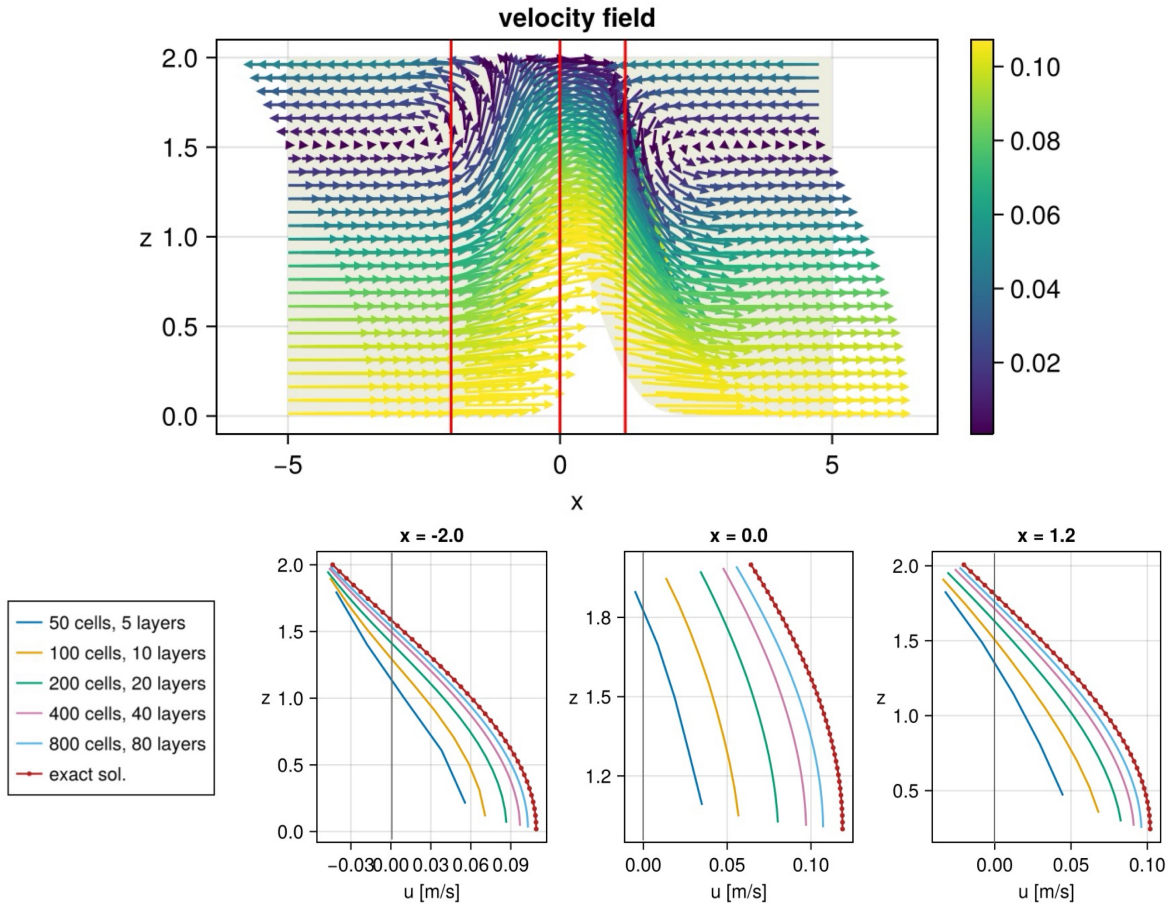

Boulanger, Bristeau, Sainte-Marie: *Comm. Math. Sci. (2013)*

Numerical Experiments – Convergence to Analytical Solution

Stationary analytical solution of Euler equations:

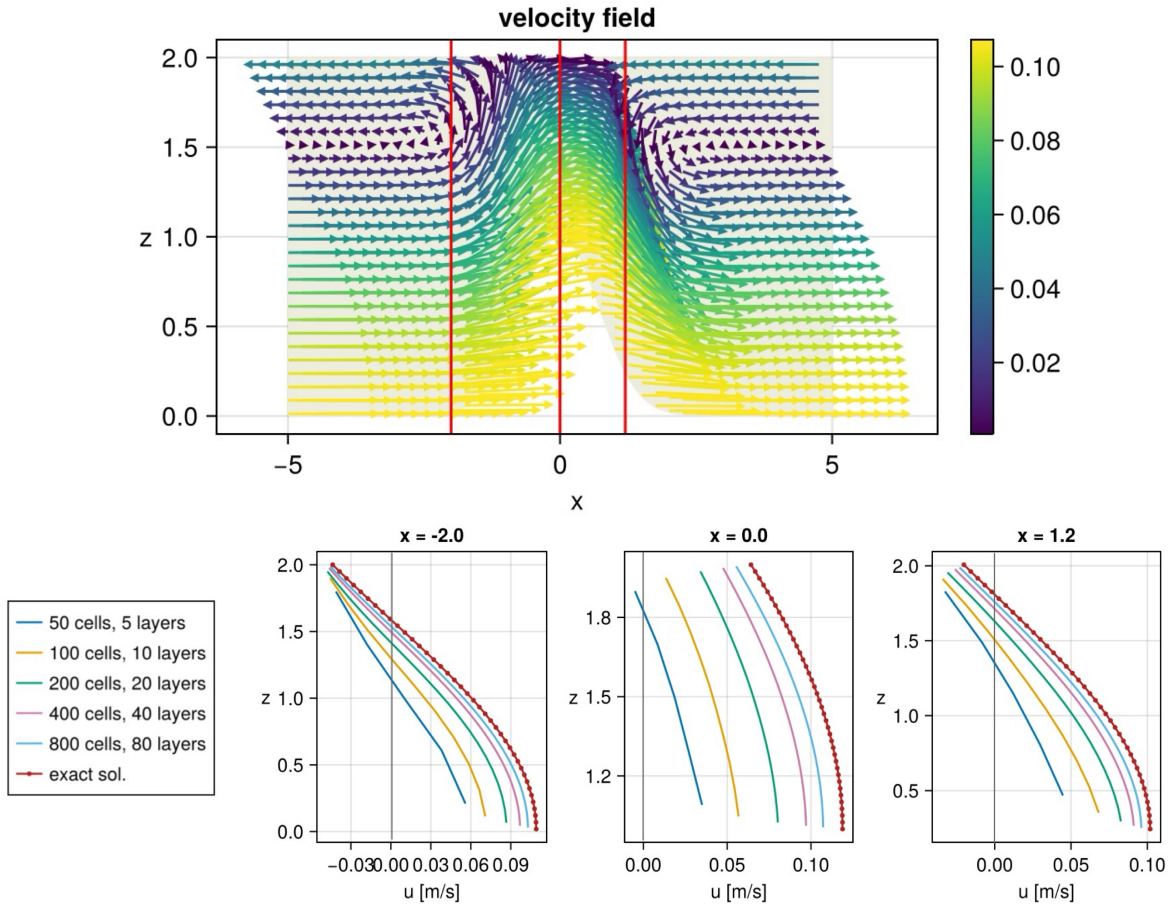

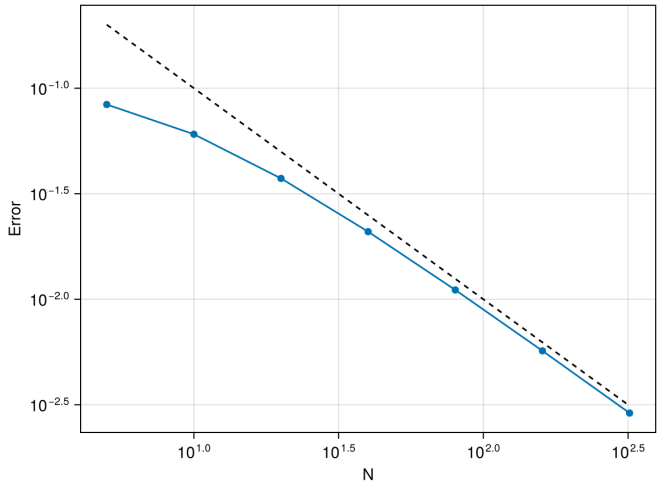

Figure: total L^1-error depending on number of layers (N) and cells ($10N$), dashed line is first order reference.

Boulanger, Bristeau, Sainte-Marie: *Comm. Math. Sci. (2013)*

Numerical Experiments – Convergence to Analytical Solution

Non-stationary Thacker bowl solution:

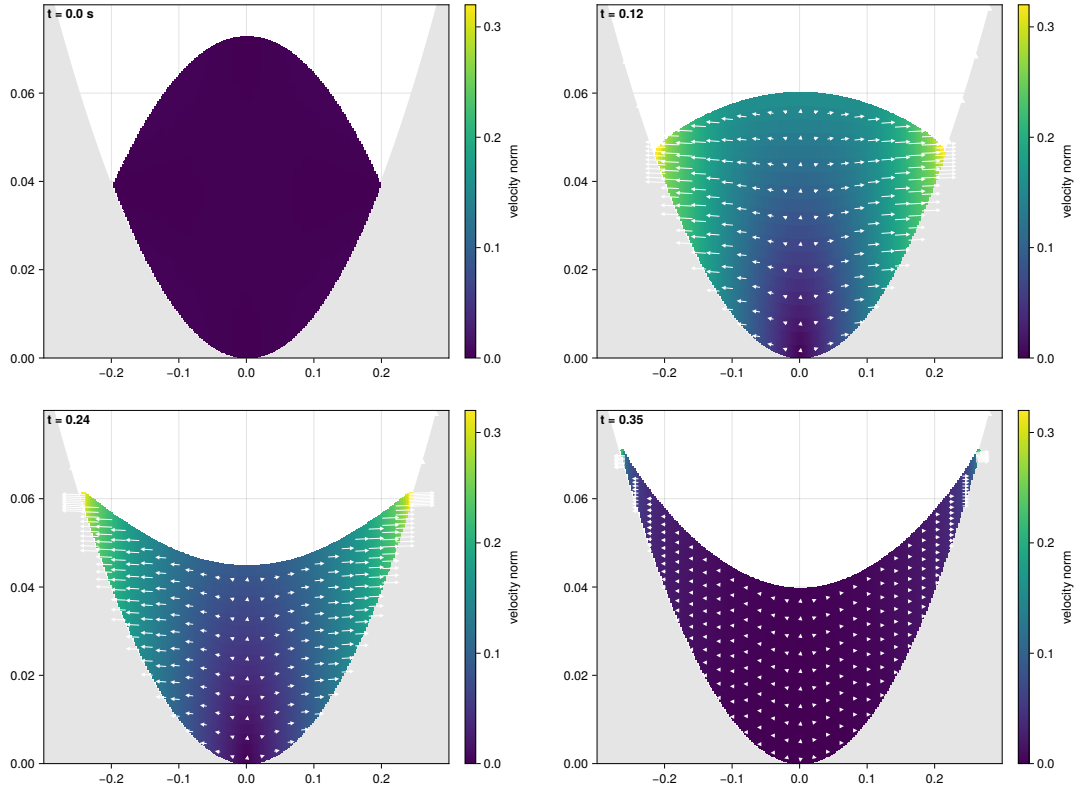

Thacker: *J. Fluid Mech. (1981)*

Numerical Experiments – Convergence to Analytical Solution

Non-stationary Thacker bowl solution:

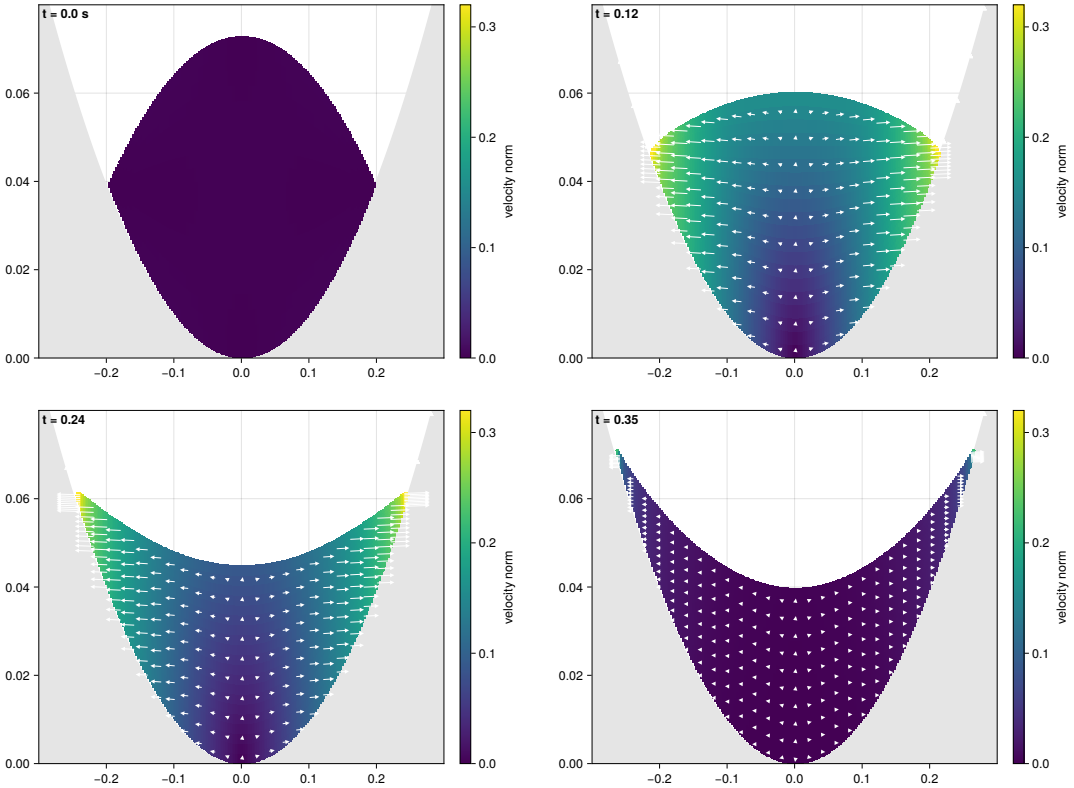

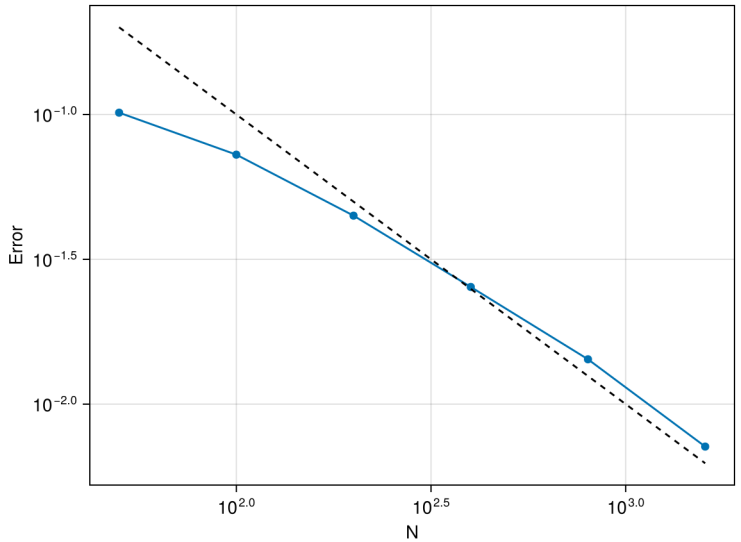

Figure: total L^1-error depending on number of layers (N) and cells ($10N \times 10N$), dashed line is first order reference.

Thacker: *J. Fluid Mech. (1981)*

Energy, Entropy, and Dissipative Dynamics

igpm

RWTH AACHEN UNIVERSITY

Numerical Experiments – Computational Cost

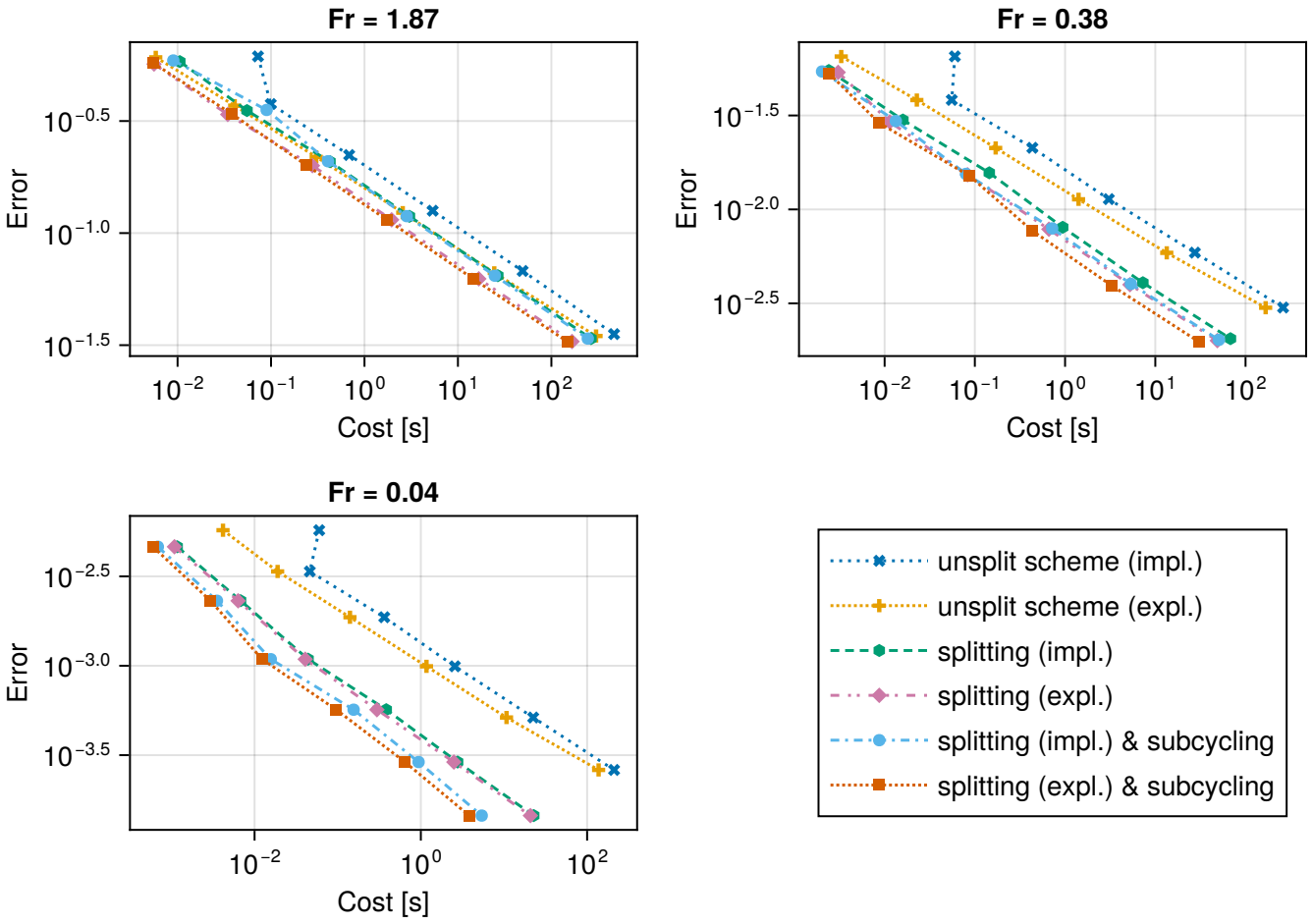

$$\mathrm{Fr} = \frac{U}{\sqrt{gH}}$$

Numerical Experiments – Computational Cost

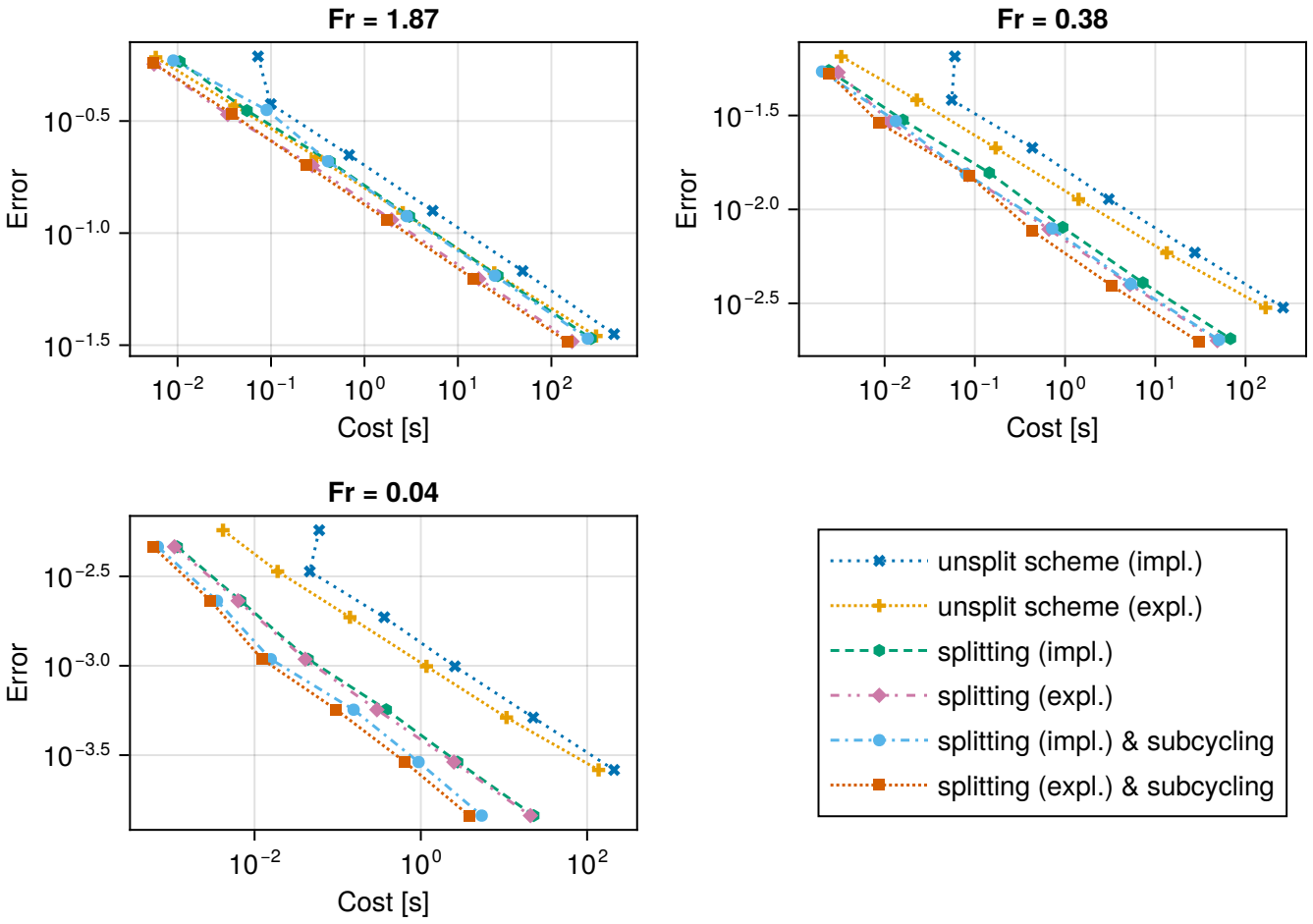

$$\mathrm{Fr} = \frac{U}{\sqrt{gH}}$$

low-Froude simulation:
100 times faster

Numerical Experiments – Computational Cost

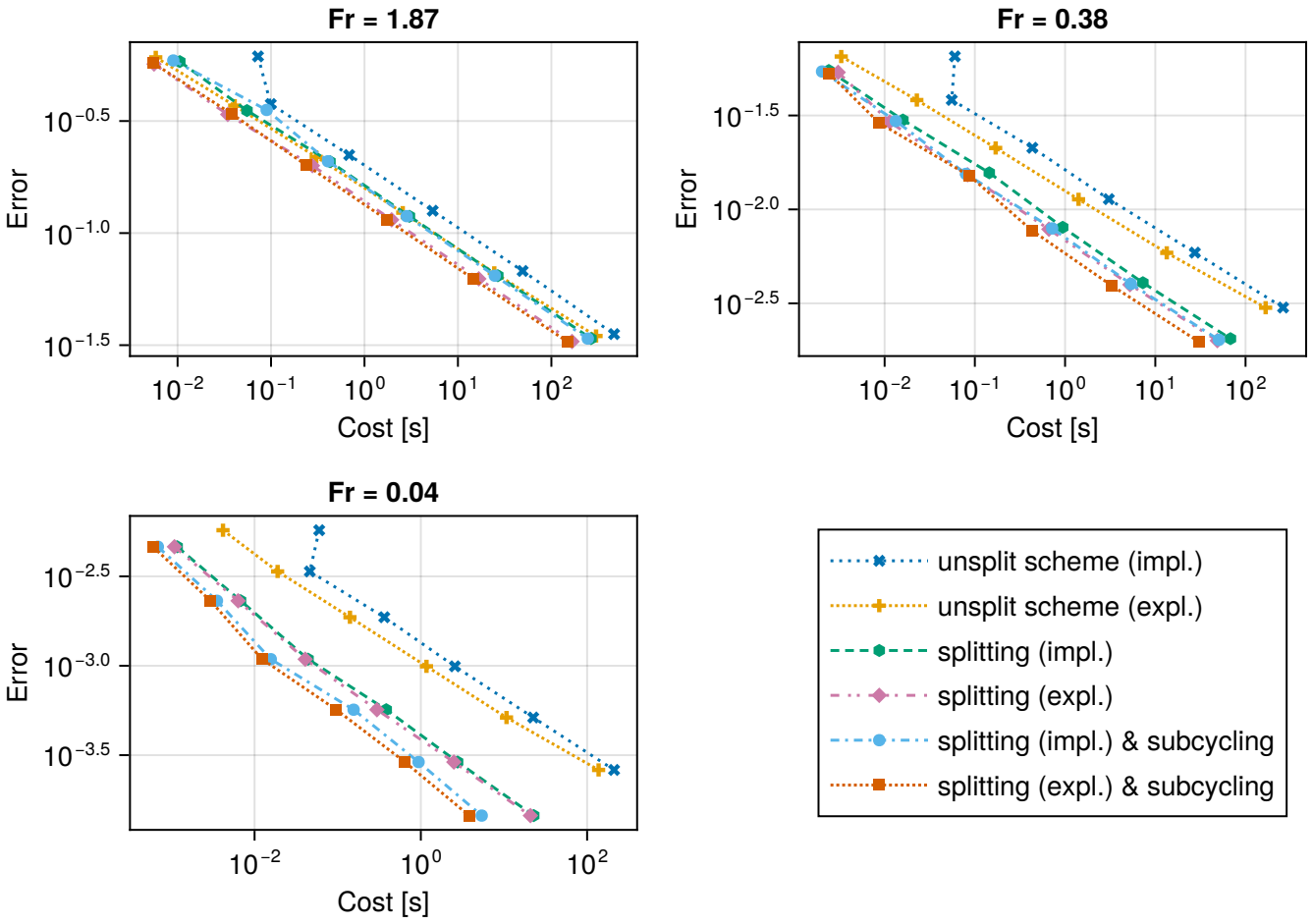

$$\mathrm{Fr} = \frac{U}{\sqrt{gH}}$$

low-Froude simulation:
100 times faster

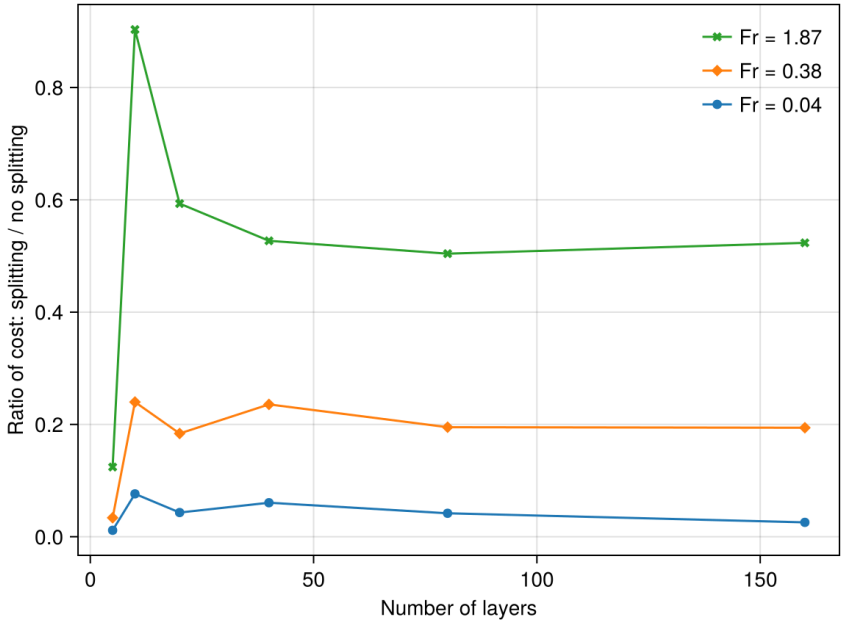

Figure: Gain in computational cost is proportional to the Froude number.

Numerical Experiments – Western Boundary Current

- ocean initially at rest
- 800×480 cells ($\Delta x = 12.5\,\mathrm{km}$), 50 layers
- wall boundary conditions
- include Coriolis force, wind forcing, bottom friction, vertical viscosity
- simulation time: 10 years

Stommel: *Transactions American Geophysical Union (1948)*
González-Tabernero, Castro Díaz, García-Rodríguez: *SEMA SIMAI Springer Ser. (2024)*

Numerical Experiments – Western Boundary Current

- ocean initially at rest
- 800×480 cells ($\Delta x = 12.5\,\mathrm{km}$), 50 layers
- wall boundary conditions

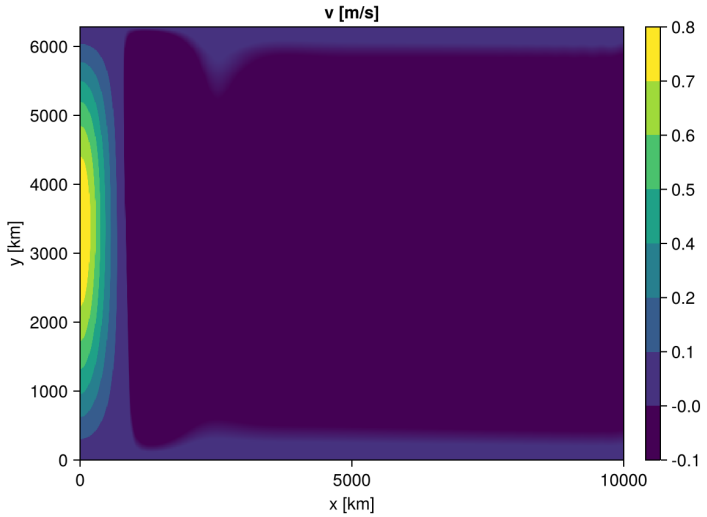

without well-balancing strategy for geostrophic equilibrium

- include Coriolis force, wind forcing, bottom friction, vertical viscosity
- simulation time: 10 years

Stommel: *Transactions American Geophysical Union (1948)*
González-Tabernero, Castro Díaz, García-Rodríguez: *SEMA SIMAI Springer Ser. (2024)*

Numerical Experiments – Western Boundary Current

- ocean initially at rest
- 800×480 cells ($\Delta x = 12.5\,\mathrm{km}$), 50 layers
- wall boundary conditions
- include Coriolis force, wind forcing, bottom friction, vertical viscosity
- simulation time: 10 years

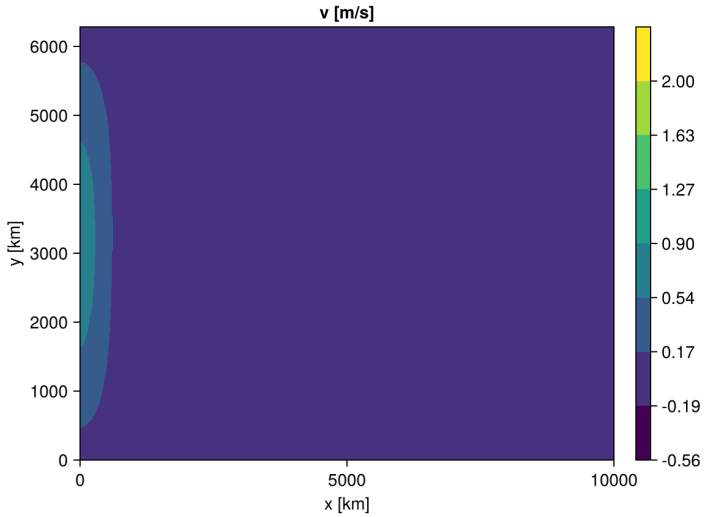

without well-balancing strategy for geostrophic equilibrium

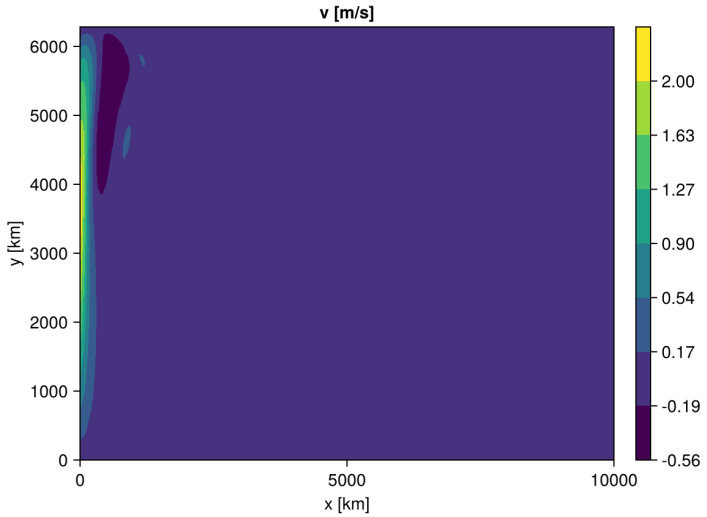

with well-balancing strategy for geostrophic equilibrium

Stommel: *Transactions American Geophysical Union (1948)*
González-Tabernero, Castro Díaz, García-Rodríguez: *SEMA SIMAI Springer Ser. (2024)*

Numerical Experiments – Western Boundary Current

- ocean initially at rest
- 800×480 cells ($\Delta x = 12.5\,\mathrm{km}$), 50 layers
- wall boundary conditions
- include Coriolis force, wind forcing, bottom friction, vertical viscosity
- simulation time: 10 years

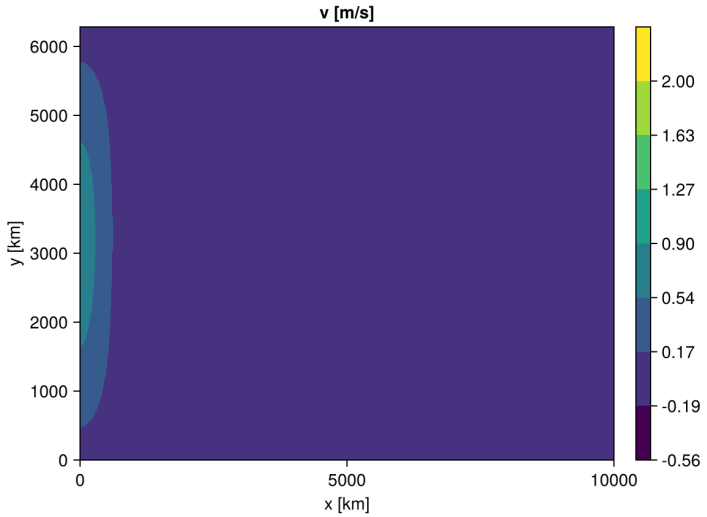

without well-balancing strategy for geostrophic equilibrium

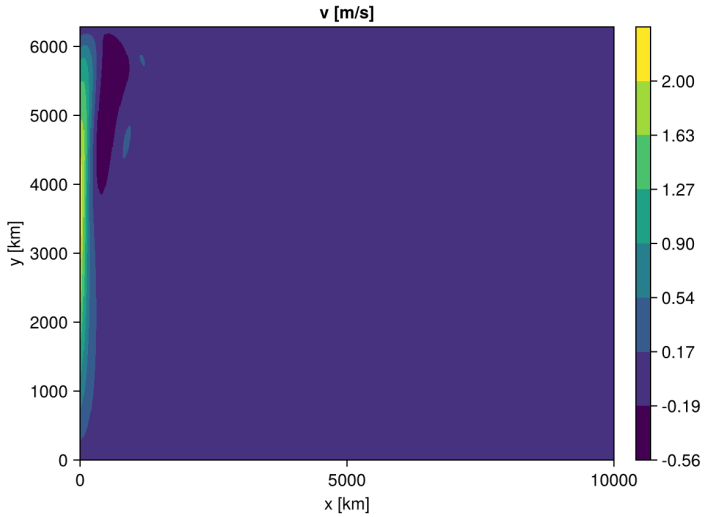

with well-balancing strategy for geostrophic equilibrium

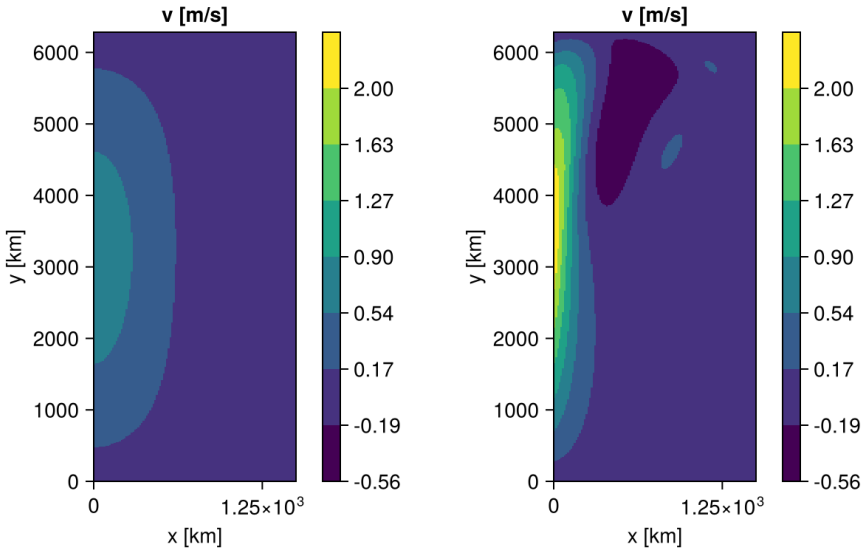

Zoom-in on western boundary current

Stommel: *Transactions American Geophysical Union (1948)*
González-Tabernero, Castro Díaz, García-Rodríguez: *SEMA SIMAI Springer Ser. (2024)*

Energy, Entropy, and Dissipative Dynamics
igpm
RWTH AACHEN UNIVERSITY

Summary and Outlook – Current and Future Work

Summary

- operator splitting strategy to reduce computational cost
- properties at continuous level:
  - hyperbolic (baroclinic: only prediction step)
  - splitting of entropy equality
- properties at discrete level:
  - non-negativity of water height and tracer concentrations
  - well-balancing inherited of the shallow water solver
  - discrete entropy inequality

Outlook

- investigate variable density case: stratification
- second order scheme

Summary and Outlook – Current and Future Work

Summary

- operator splitting strategy to reduce computational cost
- properties at continuous level:
  - hyperbolic (baroclinic: only prediction step)
  - splitting of entropy equality
- properties at discrete level:
  - non-negativity of water height and tracer concentrations
  - well-balancing inherited of the shallow water solver
  - discrete entropy inequality

Outlook

- investigate variable density case: stratification
- second order scheme

Thank you!

Energy, Entropy, and Dissipative Dynamics

igpm

RWTH AACHEN UNIVERSITY

Literature

- S. Allgeyer, M.-O. Bristeau, D. Froger, R. Hamouda, V. Jauzein, A. Mangeney, J. Sainte-Marie, F. Souillé and M. Vallée. *Numerical simulations of 3d hydrostatic Navier-Stokes system with free surface*. M2AN 53, 2019
- E. Audusse, M.-O. Bristeau, M. Pelanti, J. Saint-Marie, *Approximation of the hydrostatic Navier-Stokes system for density stratified flows by a multilayer model. Kinetic interpretation and numerical validation.*. J. Comp. Phys., 2011
- E. Audusse, M.-O. Bristeau, B. Perthame, J. Saint-Marie, *A multilayer Saint-Venant system with mass exchanges for shallow water flows. Derivation and numerical validation.* ESAIM: M2AN 45, 2011
- A.C. Boulanger, M.-O. Bristeau, J. Sainte-Marie, *Analytical solutions for the free surface hydrostatic Euler equations.* Comm. Math. Sci. Vol. 11, No. 4, pp. 993-1010, 2013
- V. González-Tabernero, M. J. Castro Díaz, J. A.García-Rodríguez. *High-order well-balanced finite volume schemes for 1d and 2d shallow-water equations with variable bathymetry and Coriolis forces*. SEMA SIMAI Springer Ser., 2024
- P. D. Killworth, D. J. Webb, D. Stainforth, S. M. Paterson. *The Development of a Free-Surface Bryan–Cox–Semtner Ocean Model.* J. Phys. Ocean., 1991
- A.J.C. Barré de Saint-Venant. *Théorie du mouvement non permanent des eaux, avec application aux crues des rivières et a l'introduction de marées dans leurs lits*. Comptes Rendus de l'Académie des Sciences, 1871
- H. Stommel. *The westward intensification of wind-driven ocean currents*. Eos, Transactions American Geophysical Union, 1948

Extension to Variable Density – Boussinesq Approximation

$\rho_\alpha = \rho_0 + \rho'_\alpha$

Baroclinic step

The baroclinic step reads

$$\begin{aligned}
&\frac{\partial h}{\partial t} = 0, \\
&\frac{\partial}{\partial t}(h_\alpha u_\alpha) + \frac{\partial}{\partial x}\left(h_\alpha u_\alpha \sigma_\alpha + \frac{1}{\rho_0} h_\alpha p'_\alpha\right) \\
&\qquad = u_{\alpha+\frac{1}{2}} G_{\alpha+\frac{1}{2}} - u_{\alpha-\frac{1}{2}} G_{\alpha-\frac{1}{2}} + \frac{1}{\rho_0}\left(p'_{\alpha+\frac{1}{2}} \frac{\partial}{\partial x} z_{\alpha+\frac{1}{2}} - p'_{\alpha-\frac{1}{2}} \frac{\partial}{\partial x} z_{\alpha-\frac{1}{2}}\right), \quad \alpha = 1, \dots, N
\end{aligned}$$

The layer-averaged pressure deviation p'_α and the interface pressure deviation $p'_{\alpha+\frac{1}{2}}$ are given by

$$p'_\alpha = g\left(\sum_{j=\alpha+1}^{N} \rho'_j h_j + \frac{\rho'_\alpha h_\alpha}{2}\right) \quad \text{and} \quad p'_{\alpha+\frac{1}{2}} = g \sum_{j=\alpha+1}^{N} \rho'_j h_j.$$

Discrete Entropy Inequality

CFL conditions:

$$\Delta t^n \leq \frac{\mathrm{CFL} \cdot \Delta x}{\max_{j,\alpha} |\sigma_{\alpha,j}|}, \qquad \delta t^k \leq \frac{\mathrm{CFL} \cdot \Delta x}{\max_j |\bar{u}_j \pm \sqrt{g h_j}|}$$

Theorem [AHS'26]

Suppose

- the shallow water solver satisfies a discrete entropy inequality
- in the prediction step the potential energy is non-increasing.

Under CFL conditions on Δt^n and δt^k, there exists a numerical entropy flux $F^E_{j\pm\frac{1}{2}}$ consistent with the continuous entropy flux F^E such that the barotropic-baroclinic splitting fulfills

$$E_j^{n+1} \leq E_j^n - \frac{\Delta t^n}{\Delta x}(F^E_{j+\frac{1}{2}} - F^E_{j-\frac{1}{2}}).$$

Discrete Entropy Inequality

CFL conditions:

$$\Delta t^n \leq \frac{\mathrm{CFL} \cdot \Delta x}{\max_{j,\alpha} |\sigma_{\alpha,j}|}, \qquad \delta t^k \leq \frac{\mathrm{CFL} \cdot \Delta x}{\max_j |\bar{u}_j \pm \sqrt{g h_j}|}$$

Theorem [AHS'26]

Suppose

- the shallow water solver satisfies a discrete entropy inequality
- in the prediction step the potential energy is non-increasing.

Under CFL conditions on Δt^n and δt^k, there exists a numerical entropy flux $F^E_{j\pm\frac{1}{2}}$ consistent with the continuous entropy flux F^E such that the barotropic-baroclinic splitting fulfills

$$E_j^{n+1} \leq E_j^n - \frac{\Delta t^n}{\Delta x}(F^E_{j+\frac{1}{2}} - F^E_{j-\frac{1}{2}}).$$

Idea of the Proof:

- prove discrete entropy inequality for each of the three steps of the splitting

Baroclinic prediction step:

- consider increment of kinetic energy
- define kinetic entropy flux by upwinding
- use definition of prediction step
- factorize and rearrange terms
- for each case proof inequality by using positivity condition on the mass flux

Energy, Entropy, and Dissipative Dynamics
igpm
RWTH AACHEN UNIVERSITY

Numerical Experiments – Convergence to Analytical Solution

Stationary solutions of the 2d (x, z) hydrostatic and incompressible Euler equations:

$$
\begin{aligned}
b(x) &= \bar{b} - H_0(x) - \frac{\alpha^2\beta^2}{2g\sin^2(\beta H_0(x))}, \\
u(x,z) &= \frac{\alpha\beta}{\sin(\beta H_0(x))}\cos(\beta(z - b(x))), \\
w(x,z) &= \alpha\beta\left(\frac{\partial b}{\partial x}\frac{\cos(\beta(z-b(x)))}{\sin(\beta H_0(x))} + \frac{\partial H_0}{\partial x}\frac{\sin(\beta(z-b(x)))\cos(\beta H_0(x))}{\sin^2(\beta H_0(x))}\right)
\end{aligned}
$$

for $\alpha, \beta \in \mathbb{R}$ and $H_0 \in C^1(\Omega)$ non-negative such that $\sin(\beta H_0(x)) \neq 0$ for all $x \in \Omega$.

We choose:

- domain $\Omega = [-5, 5]$
- $\alpha = 0.1$, $\beta = 1$, $\bar{b} = 2$
- $H_0(x) = 2 - e^{-x^2}$

and compute until final time $T = 60\,\mathrm{s}$.

Boulanger, Bristeau, Sainte-Marie: *Comm. Math. Sci. (2013)*

Energy, Entropy, and Dissipative Dynamics
igpm
RWTH AACHEN UNIVERSITY

Numerical Experiments – Convergence to Analytical Solution

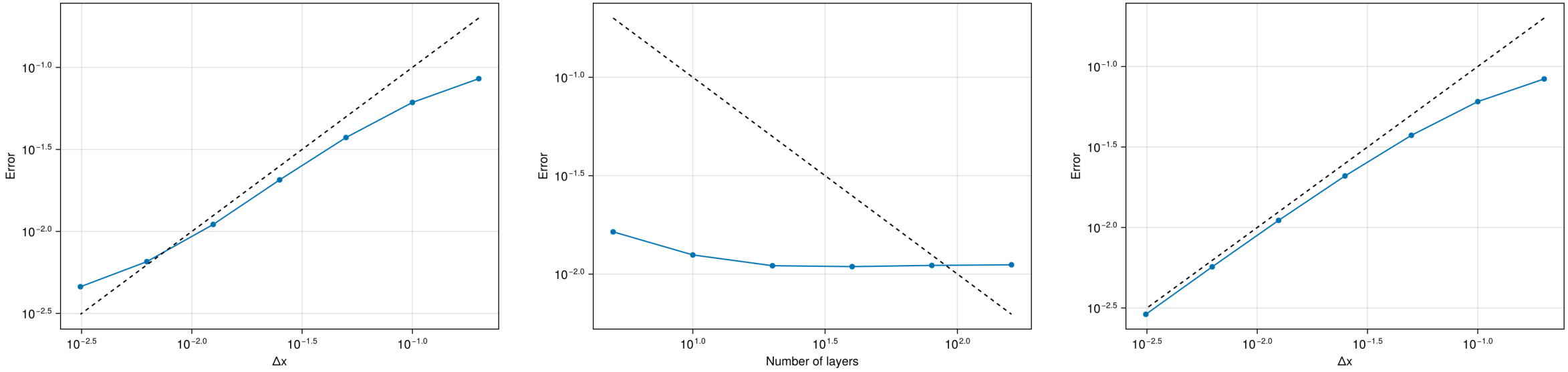

cell refinement only | layer refinement only | both, cell and layer refinement

Figure: total L^1-error depending on number of cells (left), layers (middle) and both (right), dashed line is first order reference.

Numerical Experiments – Well-balancing for Lake at Rest

We consider the computational domain $[0,4] \times [0,2]$. The initial data is given by

$$
\begin{aligned}
r(x,y) &= 2(x-2)^2 + 4(y-1)^2, \\
b(x,y) &= \begin{cases} 1 - 0.8\exp(-r(x,y)), & r(x,y) \leq \ln\frac{8}{5} \\ 0.8\exp(-r(x,y)), & \text{else} \end{cases} \\
h(x,y) &= \begin{cases} \max(0.45 - b(x,y), 0), & r(x,y) \leq \ln\frac{8}{5} \\ \max(0.3 - b(x,y), 0), & \text{else} \end{cases} \\
u &\equiv 0, \quad v \equiv 0
\end{aligned}
$$

We perform the simulation on a grid of 200×200 cells and with 10 layers until final time $T = 2$.

Chen, Noelle: *J. Comput. Phys. (2022)*

Numerical Experiments – Well-balancing for Lake at Rest

Well balanced

A scheme is called *well-balanced* if it is able to preserve steady states with machine precision.

Lake at Rest:

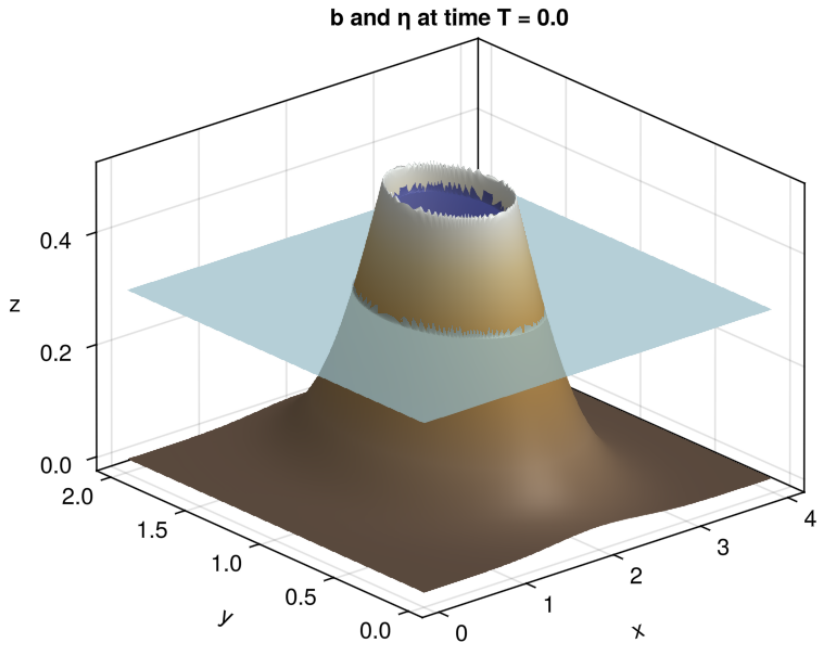

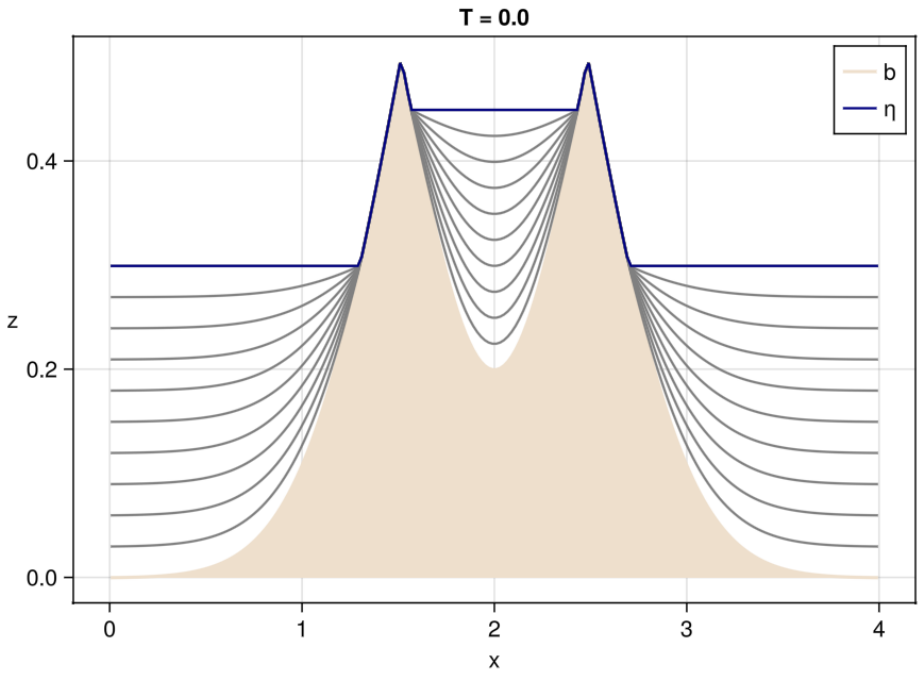

Chen, Noelle: *J. Comput. Phys. (2022)*

Numerical Experiments – Well-balancing for Lake at Rest

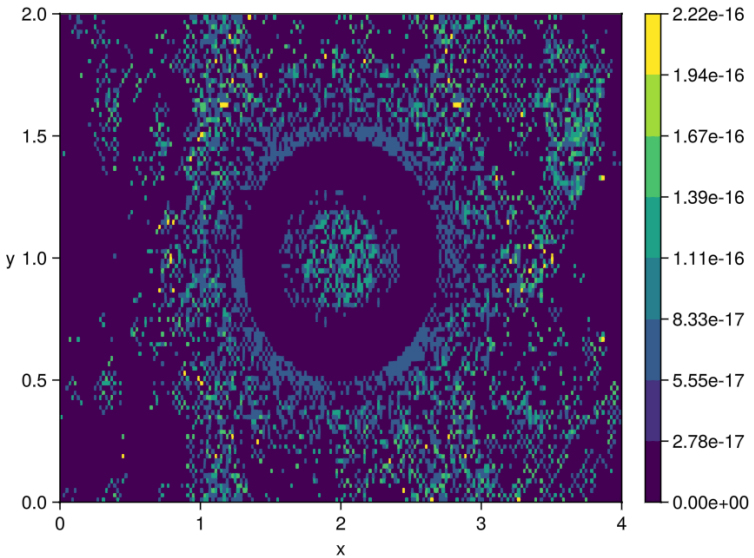

Error of free surface η.

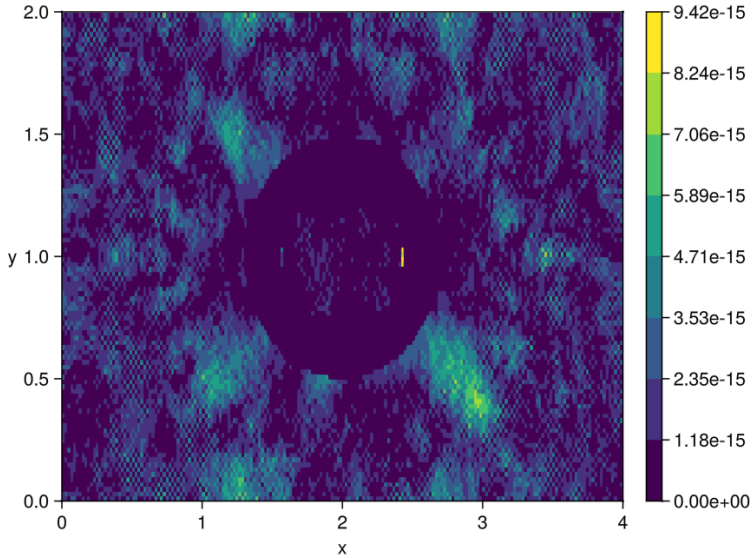

$|\sum_{\alpha=1}^{N} u_\alpha|$.

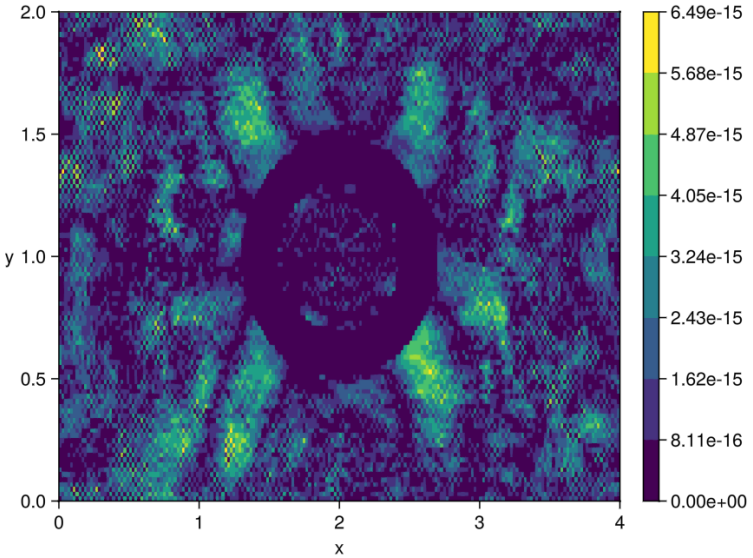

$|\sum_{\alpha=1}^{N} v_\alpha|$.

Numerical Experiments – Wind Driven Cavity

- two-layer fluid flow, initially at rest, subject to wind stress
- computational domain: $[0, 3]$, reflecting boundary conditions
- constant uniform wind stress in x-direction
- Initially the fluid is at rest with a total water height of $h = 1\,\mathrm{m}$. The initial temperature (tracer) distribution is given by

$$T_0(x, z) = \begin{cases} 25, & \text{if } z - b \geq \frac{h}{2} \\ 8, & \text{otherwise.} \end{cases}$$

- vertical viscosity: $\nu = 0.003\,\mathrm{m}^2\mathrm{s}^{-1}$
- bottom friction coefficient: $\kappa = 0.1\,\mathrm{ms}^{-1}$
- wind velocity: $6\,\mathrm{ms}^{-1}$
- final time: $t = 600\,\mathrm{s}$

Audusse, Bristeau, Pelanti, Sainte-Marie: *J. Comp. Phys. (2011)*

Numerical Experiments – Wind Driven Cavity

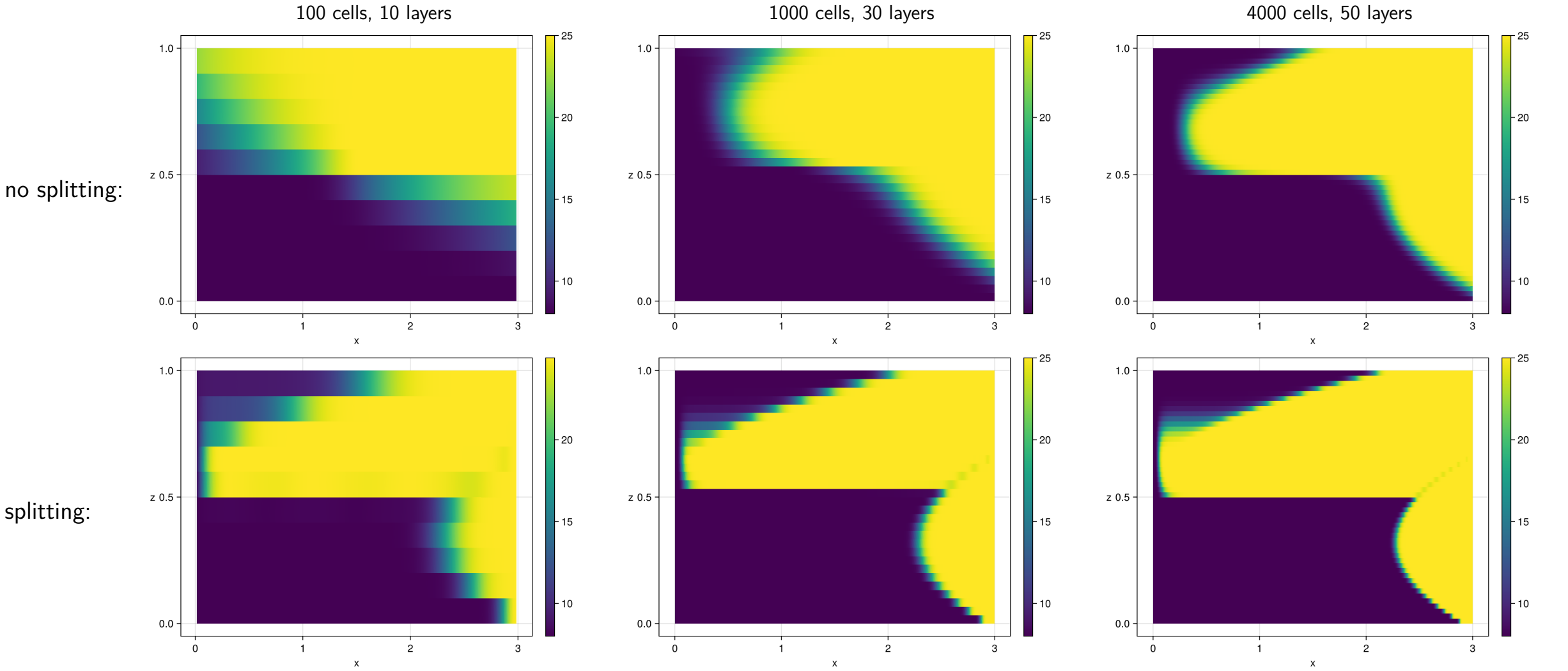

Energy, Entropy, and Dissipative Dynamics

igpm

RWTH AACHEN UNIVERSITY

Numerical Experiments – Western Boundary Current

Exact linearized solution of Stommel

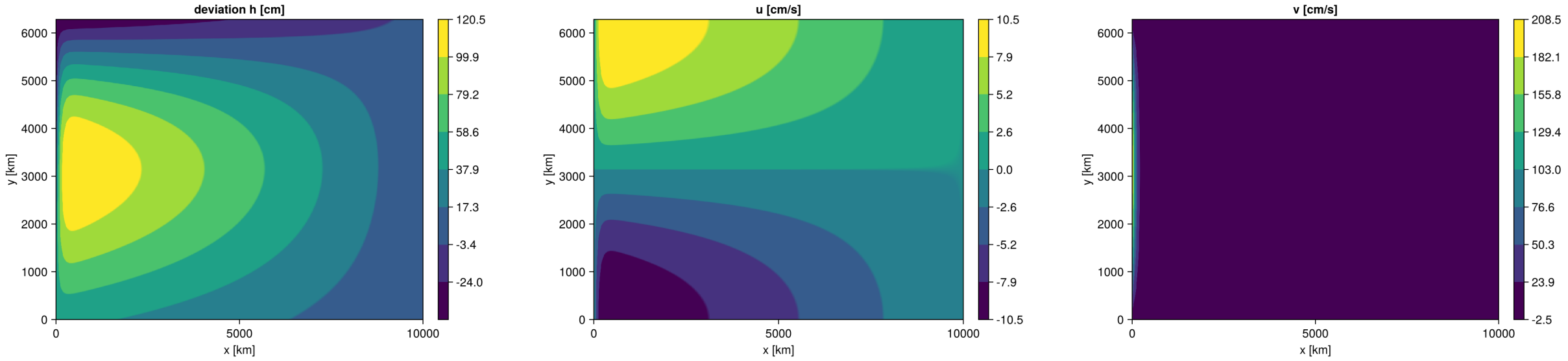

- maximum speed of western boundary current: $2\,\mathrm{m/s}$
- width of western boundary current: less than $100\,\mathrm{km}$

Stommel: *Transactions American Geophysical Union (1948)*

Numerical Experiments – Western Boundary Current

Total water height h. | Averaged zonal velocity u. | Averaged meridional velocity v.

no well-balancing:

well-balancing:

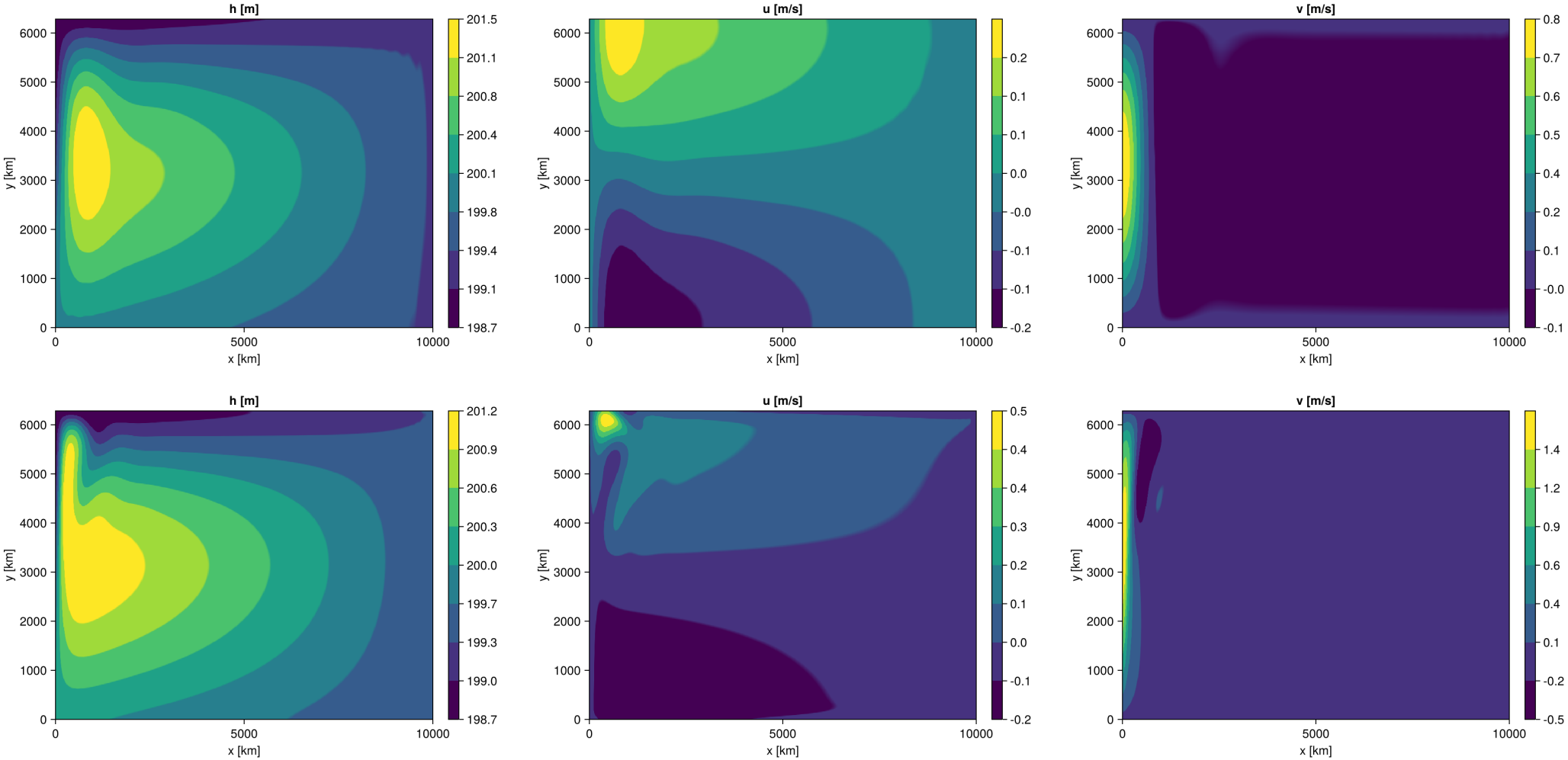

Energy, Entropy, and Dissipative Dynamics

igpm

RWTH AACHEN UNIVERSITY